Arroyo Gutierrez, Hugo (2025) *Understanding the link between mutations in the enzyme PDE10A and hyperkinetic movement disorders.* MSc(R) thesis.

https://theses.gla.ac.uk/85433/

Copyright and moral rights for this work are retained by the author

A copy can be downloaded for personal non-commercial research or study, without prior permission or charge

This work cannot be reproduced or quoted extensively from without first obtaining permission from the author

The content must not be changed in any way or sold commercially in any format or medium without the formal permission of the author

When referring to this work, full bibliographic details including the author, title, awarding institution and date of the thesis must be given

Enlighten: Theses
https://theses.gla.ac.uk/
research-enlighten@glasgow.ac.uk

Understanding the link between mutations in the enzyme PDE10A and hyperkinetic movement disorders.

Hugo Arroyo Gutierrez

Master of Science (R)(MVLS)

June 2025

Abstract

The regulation of cyclic nucleotide levels, particularly by Phosphodiesterase 10A (PDE10A), is critical for neurological function, and its dysregulation is implicated in hyperkinetic chorea-like disorders such as Huntington's Disease (HD). While PDE10A inhibition has been explored as a therapeutic strategy, clinical trials have yielded limited success, suggesting a more complex pathology than previously understood. Recent studies on PDE10A mutants propose that a loss of PDE10A function, rather than compensatory downregulation, may contribute to these symptoms.

This investigation uses biochemical techniques to characterize five newly identified human PDE10A mutants (A530T, Asn838AlafsTer46, E890D, R182Ter, and D1023_N1024insY), four of which are pathogenic and one (E890D) is non-pathogenic. Using immunoblotting, RT-qPCR, and confocal microscopy in HEK293T cells, I assessed protein expression, mRNA levels, subcellular localization, and PDE enzyme activity. Our findings reveal that the pathogenicity of early termination mutants, R182Ter and Asn838AlafsTer46, is not fully clear, and caused either by a lack of key functional domains or due to NMD degrading the mRNA of these mutants. In contrast, other pathogenic mutants (A530T and D1023_N1024insY) exhibited normal expression and localization, but showed a profound loss of phosphodiesterase activity

List of contents

Lay Summary

Phosphodiesterase 10A (PDE10A) is an important enzyme in the brain, particularly in areas that control movement. When PDE10A doesn't work correctly, it can lead to severe movement disorders, similar to what is seen in Huntington's Disease. Past attempts to treat these conditions by blocking PDE10A have not been very successful, suggesting that the problem might be more complex than initially thought.

Our study investigated specific mutations in PDE10A found in patients with these movement disorders. We discovered that these mutations can lead to the problem in two main ways: either the brain doesn't produce enough PDE10A protein, or the protein it does produce is faulty and can't perform its job effectively. Both scenarios ultimately result in a loss of PDE10A's function.

This finding is significant because it challenges a previous idea that the body might try to compensate for the disease by reducing PDE10A levels. Instead, our research suggests that a direct loss of PDE10A function is what drives the symptoms of these hyperkinetic disorders. Understanding these different ways in which PDE10A can malfunction is vital. It means that future treatments might need to be more tailored, focusing on the specific type of PDE10A defect present, rather than using a one-size-fits-all approach. This knowledge brings us closer to developing more effective therapies for these debilitating conditions.

Introduction

Cyclic nucleotides, such as cAMP and cGMP are key secondary messengers that intervene in many cellular processes, ranging from gene transcription and protein expression to cell growth, and neuronal function (D. Lee, 2015; Mayr & Montminy, 2001; Schmitt & Stork, 2001). cAMP together with its binding partner protein kinase A (PKA) plays a crucial role in the excitability of motor neurons, and the overall synaptic plasticity of the Central Nervous System (CNS) (D. Lee, 2015). There is an established link between the onset of movement disorders and the dysregulation of cyclic nucleotide levels, where mutations in key GPCR machinery, the enzymes responsible for second messenger synthesis, and their degradation are associated with these neurological disorders (Galosi et al., 2022). Specifically, mutations in Adenylate cyclase 5 (ADCY5) and Phosphodiesterase 10A, two enzymes responsible for the synthesis and degradation of cAMP respectively, have been recognised as causes of various dyskinesias (Carecchio & Mencacci, 2017). These mutants have similar phenotypical presentations to different ones in other genes, such as ATP1A3, FOXG1, NKX2.1, SLC2A1 and GNAO1, with all of them resulting in hyperkinetic chorea-like movements (Perez-Dueñas et al., 2022). When looking at certain ADCY5 gain of function mutants, these lead to a massive increase in cAMP levels due to increased levels of activity from the enzyme, which has been established as the mechanism for ADCY5-related dyskinesia (Doyle et al., 2019). The regulation of cyclic nucleotide levels has also been found to be a crucial component in the development of hyperkinetic, chorea-like disorders such as Huntington’s Disease (HD) (Gines et al., 2003).

As mentioned previously, Phosphodiesterase 10A (PDE10A) is a key enzyme involved in cyclic nucleotide signalling, where it regulates cAMP levels through the degradation of the phosphodiester bonds in the cAMP molecule (Loughney et al., 1999). Although PDE10A is expressed in many tissues throughout the body, it is most relevant to the medium spiny neurons (MSNs) in the striatum of the basal ganglia, responsible for the coordination of organised movement

(Russwurm et al., 2015). PDE10A is mainly expressed in the MSNs of the striatum, where its hydrolysing activity towards cyclic nucleotides is crucial for the control of motor function (Xie et al., 2006). It has been documented that PDE10A mutations result in aberrant cAMP signalling, leading to the improper hydrolysis of cyclic nucleotides, and allowing their concentration to rise aberrantly, and resulting in the dysregulation of key pathways in MSNs (Russwurm et al., 2015).

MSNs are dopaminergic neurons, due to the presence two families of dopamine receptors, these being the D1 and D2 families of dopamine rceptors. (Chappie et al., 2012). Generally, D1 and D2 receptors are differentially expressed, with the two receptors usually being present on different MSN populations, albeit there are smaller subpopulations that co-express both receptors. D1-MSNs are responsible for the direct pathway of the basal ganglia, which is responsible for promoting movement (Gerfen, 2023). D1 neurons are activated by the glutamate released by cortical neurons, and the dopamine released by the Substantia Nigra Pars Compacta (SNc) (Surmeier et al., 2007). Glutamate binds to a series of receptor such as AMPA and NMDA, which lead to an influx of ions and depolarisation of the membrane (Tong & Gibb, 2008). Dopamine binds to the D1 receptor, which itself forms part of a GPCR complex, resulting in the activation of adenylyl cyclase (AC) (Jones-Tabah et al., 2022). AC then begins the synthesis of cAMP, which binds to PKA, activating it, and allowing to phosphorylate further targets like L-type calcim channels, DARPP-32 or the NMDA R1 and AMPAGluA1 subunits, increasing the excitatory response (Threlfell & West, 2013). Activated D1-MSNs will release GABA onto the globus pallidus internal segment (GPi) and the substantia nigra pars reticulata (SNr), which has an inhibitory effect on their activity (Wei et al., 2016). In normal conditions the GPi and SNr have an inhibitory effect on the ventral lateral (VL) and ventral anterior (VA) nuclei of the thalamus through the release of GABA, but once these regions are inhibited these nuclei become active again (Lanciego et al., 2012). This double negative allows for the thalamus activating various regions of the motor cortex via glutamate, which then after activation starts the signal that allows for movement.

Meanwhile, D2-MSNs engage in the indirect pathway of the basal ganglia, responsible for the inhibition of movement (Gerfen, 2023). In this case both glutamate and dopamine also bind to their respective receptors in D2 MSNs, but with a different downstream response (Surmeier et al., 2007). Additionally, in the case of D2 MSNs, dopamine results in an inhibitory response, due to the Gαi/o subunit which inhibits ACs and leads to lower cAMP levels (Ford, 2014). As such, all binding partners of cAMP experience less activation overall. Active D2 MSNs then release GABA onto the Globus Pallidus External Segment, which is responsible for the inhibition of the subthalamic nucleus via GABA (Dong et al., 2021). This double negative allows for the activation of the subthalamic nucleus, which then becomes active and releases glutamate towards the GPi and SNr, which as mentioned previously have an inhibitory effect on movement (Lanciego et al., 2012).

PDE10A inhibition has specific and different deregulatory effects in both D1 and D2 dopamine receptor signalling (Chappie et al., 2012). In D1 type MSNs PDE10A inhibition leads to increased levels of PKA signalling due to higher baseline cAMP levels, that are the result of a lack of PDE activity. These D1 type neurons are then less sensitive to dopamine stimulation, due to the already high levels of cAMP in the cell, so that adenylyl cyclase activation via D1 receptor activation does not result in a notable increase of cAMP in the neuron, due to the ceiling imposed by PDE10A being removed (Sotty et al., 2009). In the case of D2 type MSNs inhibition of PDE10A also leads to increased levels of cAMP due to a lack of degradative activity. Downstream signalling of the D2 type dopamine receptors is less effective when PDE10A is inhibited, due to higher-than-average levels of cAMP in the neurons, resulting in a hindered response due to floor set by PDE10A being removed (Mota et al., 2021). Despite activation of the D2 pathway, which is responsible for cAMP degradation, the already high cAMP levels lead to a smaller overall impact in total concentration in the cell. Such effects are especially noticeable after the activation of A2A adenosine receptors (commonly co-expressed in D2 type MSNs), which similarly to D1 dopamine receptors, also lead to increased levels of cAMP in MSNs (Heckman et al., 2016). As such, inhibition of PDE10 results

in aberrant dopamine signalling in D1 and D2 type MSNs, leading to increased cAMP levels and PKA signalling in the vast majority of the basal ganglia (Mota et al., 2021).

PDE10A contains three major domains in its structure, those being GAF-A, GAF-B, and its catalytic domain (García et al., 2017). The catalytic domain of PDE10A is dual specific, having an affinity both towards cAMP and cGMP, although specificity towards cAMP relative to cGMP is considerably higher, with the K_m of PDE10A for cAMP being 0.26 μM and the K_m for cGMP being 7.2 μM. Nonetheless PDEA10A exhibits a much higher V_{max} for cGMP than it does for cAMP, with cGMP having a V_{max} of 1.4 pmol/min/μg and cAMP having a V_{max} of 0.63 pmol/min/μg (Fujishige et al., 1999). Additionally, cAMP has a stimulatory effect on cGMP processing by PDE10A, where cGMP hydrolysis activity increases up to 25% when in the presence of cAMP up to a concentration of 0.1 μM, with 0.1 μM being the concentration at which the highest level of stimulation is reached. Nonetheless concentrations of cAMP higher than 0.1 μM have inhibitory effects, with 1 μM causing a notable decrease in enzymatic activity (Fujishige et al., 2000). The GAF-A domain in PDE10A is responsible for its correct subcellular localisation, as it allows for the palmitoylation of PDE10A and its integration into the membrane of the cell. It is speculated that GAF-A possesses a binding region for the enzyme palmitoyl transferase (zDHHC), which is responsible for the palmitoylation of a further cysteine residue (C11) on the N-terminus of the protein (Tejeda et al., 2020). The GAF-B domain of PDE10A is responsible for its binding with cAMP in a cGMP stimulatory manner, additionally, GAF-B is also responsible for the correct dimerization of PDE10A (Handa et al., 2008). Dimerization occurs via a series of hydrophobic interactions between bundled helices present in the GAF-B domains from two separate PDE10A proteins in an asymmetric manner. Here the helices present in the GAF-B domain of one protein interact with a different helix in the GAF-B domain of the other PDE10A protein (for example helices α1 and α2 of molecule A bind with helix α5 of molecule B, instead of the helices α1 and α2) (Handa et al., 2008). The catalytic domain of PDE10A is responsible for its phosphodiesterase activity, hydrolysing the phosphodiester bonds in its

substrates. Double specificity is achieved through the substrate's interaction with key amino acids (where Gln726 interacts directly with the substrate) and two divalent metals (magnesium and zinc) that coordinate with these amino acids (Lau et al., 2010). Additionally, depending on the splice variant, the N terminus of PDE can act as a region for post translational modifications, here are the palmitoylation site (Cys11) and, and a threonine residue (Thr16) which acts as a phosphorylation site that regulates PDE10A activity (Charych et al., 2010; Jäger et al., 2012).

PDE10A has three prevalent isoforms, which share the three key domains previously described, these splice variants are PDE10A1, PDE10A2, and the recently discovered PDE10A19, found to be exclusive in primates (Macmullen et al., 2016; Russwurm et al., 2011) . Out of these PDE10A isoforms only PDE10A2 is commonly translocated to the membrane, while PDE10A1 and PDE10A19 are most commonly found in the cytosol, this is due to their alternatively spliced N-terminal sequences lacking the necessary cysteine residue that gets palmitoylated in PDE10A2 (Kotera et al., 2004). Increased expression of PDE10A19 has been found to change the localisation of PDE10A2 from the membrane to the cytoplasm, as co-immunoprecipitation experiments confirm that the two different isoforms physically interact with each other. Although it is common for the vast majority of PDE families to form homodimers, and in some cases heterotetramers, this recent evidence suggests that PDE10A2 and PDE10A19 are able to form heterodimers (Macmullen et al., 2016; Russwurm et al., 2015). Due to the potential of dimerisation it is thought that variation in the expression of PDE10A19 is able to change the PDE activity in the membranes of neurons by removing PDE10A2 out of the membrane into the cytoplasm. This would represent an additional pathway in which cAMP levels are spatially regulated.

Newly discovered mutations in the PDE10A gene have shed some light on the key role the enzyme plays in motor function (Whiteley et al., 2019). PDE10A levels were found to be much lower in premanifest HD gene carriers long before

any chorea-like symptoms are manifested in patients (Wilson et al., 2016). These changes in PDE10A levels were found in the MSNs, both in the striatum and globus pallidus in the basal ganglia (Niccolini, Foltynie, et al., 2015). Because of these findings, it was assumed that cAMP and cGMP signalling is a key aspect to development of HD, and that a disruption in cyclic nucleotide levels is a crucial event in the onset of the disease. Additionally, it was also found that contrary to the striatum and globus pallidus, PDE10A levels increased in the thalamic nuclei in HD premanifest gene carriers (Niccolini, Haider, et al., 2015). It was shown that the specific region in the basal ganglia which suffered the most notable decrease in PDE10A levels was the striatum, and that one of the biggest deciding factors for the development of the disease was the ratio in PDE10A being expressed in the neurons forming the striatopallidal projecting striatum (part of the striatum that sends output to the globus pallidus) relative to the thalamic nuclei. Lower levels of PDE10A in the striatum relative to those in the thalamic nuclei have been found to be a strong predictor of the transition between non-manifesting to manifesting HD in the carrier (Niccolini, Haider, et al., 2015). These findings regarding PDE10A levels in the basal ganglia have been instrumental for directing and focusing research on PDE10A as therapeutic target. One of the more commonly accepted hypotheses when understanding the role PDE10A during progression of HD is that PDE10A levels are altered in a compensatory manner in order to allow for correct cyclic nucleotide signalling, and that once past a certain threshold, onset of the disease appears (Niccolini, Haider, et al., 2015).

In this light, the transition of non-manifesting to manifesting carriers of the HD gene thought to be mediated by an inability of the basal ganglia to maintain healthy cyclic nucleotide levels through the regulation of PDE10A expression and activity.

Another key aspect to consider for the pathogenesis of HD, and where PDE10A might intersect, is the interactions that the aberrant form of the protein huntingtin (mHtt) has with a series of key proteins for cell signalling. Htt has the

ability to bind to CREB binding protein (CBP), through its pathogenic region located in exon 1 (httex1p), a key transcriptional coactivator for the correct functioning of neurons (Cardinaux et al., 2000). When mHtt binds to CBP it is able to sequester the coactivator within the aggregates it forms, disrupting downstream signalling (Wanker et al., 2019). As its namesake indicates, CBP takes part in cAMP responsive element-binding protein (CREB) signalling as a coactivator. CREB signalling begins with the activation of either adenylyl cyclase or guanylyl cyclase, responsible for the production of cyclic nucleotides cAMP and cGMP, which bind to either Protein Kinase A (PKA) or Protein Kinase G (PKG) (Wang et al., 2018). Both kinases are responsible for the phosphorylation of CREB, and its activation. CREB signalling is responsible for the transcription of Brain-Derived Neurotrophic Factor (BDNF), a protein crucial for the survival and development of striatal neurons (Miniaci et al., 2024). Such a decrease in CREB signalling is compounded with cAMP levels in patients of HD, especially at death, having been found to be lower than in healthy individuals (Gines et al., 2003). This hypothesis acts as the basis behind the vast majority of therapies that hold PDE10A as their focal point, seeking to inhibit the protein. The rationale behind this hypothesis is that by inhibiting PDE10A, the base level of cyclic nucleotides cAMP and cGMP in neurons increases, for which there is robust and established experimental evidence (Beaumont et al., 2016). This increase in concentration of secondary messengers would lead to increased activation of PKA and PKG, the rise in activity of the kinases would increase the amount of phosphorylated CREB protein, which should allow for higher baseline active CREB (Menniti et al., 2021). This hypothesis nonetheless does not account for the fact that, as explained above, PDE10A levels vary in opposite trends depending on the region in the basal ganglia. As it was previously reported, PDE10A levels do decrease in the striatum in the basal ganglia in a notable way, lending credence to the fact that maybe it is a compensatory adjustment to allow for more CREB signalling and BDNF production (Niccolini, Haider, et al., 2015). While on the other hand, PDE10A levels in the thalamic nuclei experience a marked increase, as a way to keep their activity at normal levels in order to regulate the release of glutamate into the cerebral cortex. As such, inhibition of PDE10A as a way to treat HD may be a useful approach, but due to the fact that different

regions in the basal ganglia experience different kinds of regulation (downregulation in the striatum, upregulation in the thalamic nuclei) it is difficult to ascertain whether systemic pan-PDE10 inhibition will yield any results.

Phosphodiesterases have been researched as potential therapeutic targets for decades, with an emphasis on their inhibition as a way to treat disease (Baillie et al., 2019; García et al., 2017; Knott et al., 2017). PDE10A specifically has been researched as target to treat diseases and conditions of the CNS, including schizophrenia, Tourette's, Parkinson's Disease, Huntington's Disease (Marshall et al., 2024; Niccolini, Foltynie, et al., 2015; Niccolini, Haider, et al., 2015). Additionally, links between PDE10A and mental health have in humans also been established, with the protein playing a role in the mood instability characteristic of Bipolar disorder I (BD-I) (Macmullen et al., 2016). Unfortunately, despite multiple PDE inhibitors shown having promising pre-clinical data in mice models of neurological diseases, no therapeutic solution involving inhibition of PDE10A is currently available. One example is MP-10, developed by Pfizer, which has been trialled as a possible therapeutic solution both for schizophrenia and HD. In a HD disease model based on mice, administration of MP-10 resulted in an increase of cyclic nucleotide levels (both in cAMP and cGMP) and was able to rescue basal ganglia function. When applied to non-human primates MP-10 it had a common baseline effect to other inhibitors of the D2 receptor activity in MSNs (Delnomdedieu et al., 2018; Demartinis et al., 2019).

Looking at the previously presented trials regarding PDE10A inhibitors it does not appear that inhibition has been a fruitful avenue of research, as no inhibitory molecule targeting PDE10A has proven to be an effective therapy. Nonetheless, the fact that MP-10 and many other inhibitors are still undergoing effectivity and safety trials to study their therapeutic potential, shows that this is still a relevant area of research. PDE10A is therefore regarded as a promising therapeutic target for hyperkinetic chorea-like disorders, and my study seeks to shed some light on the potential mechanisms involved (Heckman et al., 2016).

Recent studies looking at disease causing PDE10A mutants have suggested a different pathology in regard to PDE10A and HD, or on the very least offer new insights into how hyperkinetic disorders develop in human beings (Baillie et al., 2019; Whiteley et al., 2019). It has been proven that mutations in PDE10A resulting in decreased activity or a total loss of function result in a phenotype very similar to that of HD (Knopp et al., 2019). This contradicts at least partly the previous working hypothesis, where a loss in PDE10A activity was compensatory measure taken by neurons to keep normal neuronal activity, and not the source of hyperkinetic chorea-like symptoms (Ahmad et al., 2014). Such phenotypes have been driven by mutations found both in the GAF-A and GAF-B domains in PDE10A, although the way in which the hyperkinetic chorea-like symptoms are mediated differ depending on what domain the mutation is present (Kalampokini et al., 2023; Mencacci et al., 2016). GAF-A mutants have been found to deprive the membrane of the striatum of MSNs of PDE10A, due to aberrant intra-cellular localisation of the enzyme. These GAF-A mutants are thought to be deficient in recruitment of the zDHHC enzyme necessary for the palmitoylation of the 11cys residue which would anchor PDE10A to the membrane, reducing its enzymatic activity in this compartment of the cell (Tejeda et al., 2020). GAF-B mutants are properly trafficked to the membrane of the striatum, but still are not able to function like their wild-type version. Mutations in the second GAF domain result in misfolding, may stop the protein from properly dimerising, and lead to the formation of aggresomes in the membrane (Tejeda et al., 2020; Whiteley et al., 2019). Additionally, GAF-B mutants lose the stimulatory effect on the hydrolysis of cAMP when bound to cGMP, reducing the overall activity of the protein. Change to either of these domains will result in chorea-like symptoms, putting into doubt whether the correct approach when dealing hyperkinetic disorders is PDE10 inhibition, or if a strategy that realises an upregulation in PDE10 activity might bear better results (Narayanan et al., 2018).

My investigation focuses on five newly obtained PDE10A mutants from a cohort of patients curated by clinicians at UCL, of which four have been proven to be pathogenic. The mutants in question are A530T, Asn838AlafsTer46, E890D,

R182Ter, and D1023_N1024insY. Out of these mutants A530T, N838Afs, R182Ter, and D1023_N1024insY have been proven to be pathogenic, while E890D seems to have no notable effect on those suffering the point mutation, presenting itself as non-pathogenic. Most of these mutations are located in vicinity of the catalytic domain of PDE10A, with the exception of R182Ter, which is located in the GAF-A domain, and constitutes an early termination mutation. These mutants are responsible for the development of chorea-like symptoms, similar to those of HD, and also to other mutations in PDE10A that result in a loss of function, as seen with mutations in the GAF-A and GAF-B domains. This series of new point mutations may offer more specific insights into the relationship between PDE10A, chorea, and what place PDE10A has in the onset and development of hyperkinetic disorders such as HD. In this investigation the Baillie lab has generated plasmids containing the PDE10A mutations and I have transfected into human cell lines to allow biochemical characterisation in terms of ability to be expressed, activity, cellular location, and trafficking versus wild type PDE10A.

RESULTS

PDE10A Mutant Expression in HEK239 cells and Structural Implications

Understanding the underlying changes in cellular physiology responsible for hyperkinetic symptom caused by PDE10 will be key to development of a suitable therapeutic strategy. It has already been shown that point mutations can impact PDE10A function through a multiplicity of mechanisms, all distinct from each other. Although the majority of the mutants examined in this specific study are primarily located within the catalytic domain of PDE10A, it is a common misconception to assume that all of them result in a straightforward loss of function solely due to a lack of enzymatic activity. As mentioned before, studies on mutations within the GAF-A domain of PDE10A have revealed that while these mutations may not alter the protein's overall spatial location within the cell, they instead induce misfolding, leading to the accumulation of the protein, a situation that underpins the pathogenic phenotype. On the other hand, point mutations in the GAF-B domain can directly disrupt the protein's subcellular localization, resulting in spatial dysregulation within the cell. As such, there are multiple ways in which point mutations may affect the correct functioning of PDE10A, which makes it necessary to investigate each one separately.

To achieve this, constructs of the mutants incorporating a FLAG tag on the C-terminus were generated by the Baillie lab previous to the beginning of my investigation, and subsequently expressed transiently in HEK293T cells and the cellular lysates used for immunoblotting. As depicted in Figure 1, the immunoblotting results indicated that, relative to Wild Type (WT) PDE10A, all of the mutants, with the notable exceptions of R182Ter and Asn838AlafsTer46, were expressed at comparable levels. There is a trend when looking at the FLAG immunoblots, of mutants having lower levels of expression when compared to WT, including E890D despite being non-pathogenic, albeit with the p values being close to, but still above 0.05. It is expected that a termination mutant such as R182Ter would not be detected in this situation, due to the FLAG tag in the constructs being present in the C-terminus. As the R182Ter mutation introduces a stop codon very early in the coding sequence, the

resulting truncated protein would lack both the targeted C-terminal region where the specific PDE10A and the C-terminal FLAG tag antibodies would bind (see figures 1c and 1d). The apparent lack of expression of R182Ter may be due to both of the detectable regions not being expressed. Although lack of detection may also be due to degradation of the product by the Ubiquitin-proteasome system (UPS) due to it being truncated and more likely to misfold. Similarly, Asn838AlafsTer46 also exhibited significantly lower expression levels compared to Wild Type PDE10A and all other expressed mutants (see figures 1c and 1d). This frameshift mutation is situated within the catalytic domain and results in premature termination 46 residues downstream of the mutation site. A similar problem to R182Ter arises with this construct in that the early termination likely accounts for the lack of protein detection via immunoblotting, as both antibodies used are specific to the C-terminus of PDE10A, which is also truncated in the case of Asn838AlafsTer46. This mutant may also be tagged for degradation by the UPS.

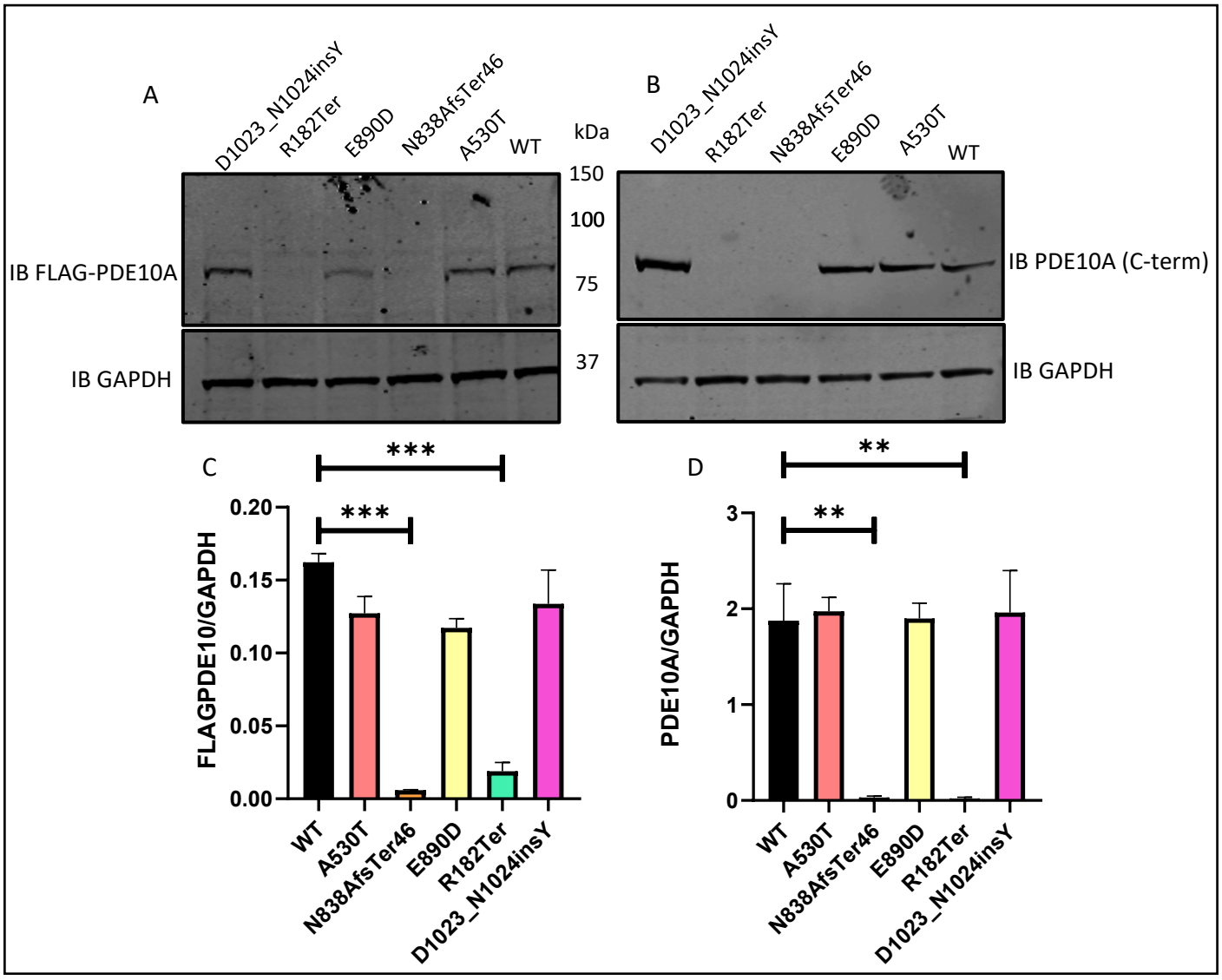

Figure 1. **Pathogenic early termination codons prevent the detection of PDE10A by immunoblotting.** (A) Immunoblot showing the protein levels of recombinant FLAG-tagged PDE10A constructs expressed in HEK293 cells. GAPDH was used as a loading control. (B) Immunoblot probing for the C-terminal region of both endogenously expressed PDE10A and transiently expressed product, with GAPDH as a loading c ontrol. (C) Quantification of FLAG-PDE10A protein levels from densitometric analysis, normalized to GAPDH Graph shows the mean ± SEM. Statistical analysis was performed by one-way ANOVA followed by Dunnett's post hoc (***P < 0.0001; n = 3). (D) Quantification of both endogenously expressed PDE10A and transiently expressed product protein levels from densitometric analysis, normalized to GAPDH. Graph s hows the mean ± SEM. Statistical analysis was performed by one-way ANOVA followed by Dunnett's post hoc (**P < 0.001; n = 3). Antibodies (1), (2), (3), (6), and (8) from Table 1 were used.

Expression Levels Do Not Universally Determine Pathogenicity

While the absence of detectable protein for early termination mutants like R182Ter and Asn838AlafsTer46 strongly suggests their direct role in pathogenicity through a profound lack of expression and inherent structural incompleteness, this explanation is not applicable to all the studied mutants. For those mutants that were consistently expressed and detected at levels comparable to wild-type PDE10A, such as the non-pathogenic E890D and the pathogenic A530T and D1023_N1024insY, detection itself seems to not be a decisive factor in determining their pathogenic outcome.

PDE10A mRNA Expression Levels

In mutations with low expression there is a possibility that this lack of protein detection via immunoblotting is due to a lower basal level of mRNA expression relative to WT PDE10A. To better characterise pathogenic mutants within the cellular environment, and to gain additional insights into the behaviour of the other mutants that were successfully detected by immunoblotting, RT-qPCR was employed. Beyond using primers designed to target both the N-terminus and C-terminus of PDE10A mRNA, the gene for Tia1 cytotoxic granule-associated RNA binding protein (TIA-1) was also targeted. TIA-1 has been previously identified as a key component that co-aggregates with mutant huntingtin (mHtt) in inclusion bodies, a process that occurs as part of an early cellular stress response (Furukawa et al., 2009). This stress response involves the formation of stress granules (SGs), and the presence of TIA-1 is indispensable for their assembly. Secondly, and particularly relevant to this study, it has been reported that in other PDE10A mutants, where affected individuals developed hyperkinetic chorea-like symptoms, PDE10A was observed to co-aggregate with TIA-1 (Tejeda et al., 2020). This co-aggregation phenomenon was specifically noted within P-bodies, which are distinct cytoplasmic structures known to be derived from SGs. These PDE10A mutants that formed aggregates were found to be misfolded, directly leading to their loss of function. A significant upregulation of TIA-1 in any of the currently investigated PDE10A mutants could serve as a potential indicator of a similar underlying mechanism contributing to the observed pathogenic phenotype.

Asn838AlafsTer46 and R182Ter Show Notably Lower mRNA Levels

Nonetheless, analysis of the expression levels for each of the targeted genes during the RT-qPCR experiments revealed very little variance from the baseline established by WT PDE10A for the majority of mutants. Crucially, none of the mutants exhibited significantly different levels of TIA-1 expression when compared to WT PDE10A (see figure 2c). This lack of differential TIA-1 expression makes it highly unlikely that the source of the observed pathogenic phenotype in these specific mutants is due to widespread protein misfolding leading to aggregation. When examining the mRNA levels for both the C-

terminus and N-terminus of PDE10A, the majority of the mutants demonstrated no significant increase or decrease in their expression levels compared to those of WT PDE10A (see figure 2). Specifically, all of the mutants that were successfully detected via immunoblotting (A530T, E890D, and D1023_N1024insY) showed practically identical mRNA expression levels to those of WT PDE10A, irrespective of whether the N-terminus or the C-terminus of the protein's mRNA was being amplified (see figures 1a and 1b).

The only notable exceptions to this trend were the two mutants that failed to produce relevant bands for either FLAG or PDE10A in the immunoblotting experiments (see figures 2a and 2b). Asn838AlafsTer46 exhibited a decreased expression for both its C-terminus and N-terminus mRNA levels relative to WT PDE10A. Quantitatively, this translated to a 0.695-fold change when comparing the N-terminus and a 0.595-fold change for the C-terminus. R182Ter also showed significantly lower levels of expression for both its C-terminus and N-terminus, following a similar trend, R182Ter experienced a 0.567-fold change in expression for the N-terminus and a 0.579-fold change for the C-terminus. Again, showing mRNA levels in the cell much lower than both the wild type PDE10A and the remaining mutants that were able to be detected via immunoblotting (see figures 1a and 1b).

The absence of significantly different TIA-1 expression across all mutants strongly suggests that widespread protein misfolding and subsequent aggregation is not a primary cause of the hyperkinetic, chorea-like pathogenic phenotype in the specific mutants investigated here. RT-qPCR results also demonstrate that the notably lower protein expression levels observed via immunoblotting for the early termination mutants, R182Ter and Asn838AlafsTer46, directly correlate with significantly reduced mRNA levels for both their N- and C-termini. Conversely, for those mutants successfully detected by immunoblotting (A530T, E890D, D1023_N1024insY), expression seems to not be a decisive factor in determining their pathogenic or non-pathogenic nature.

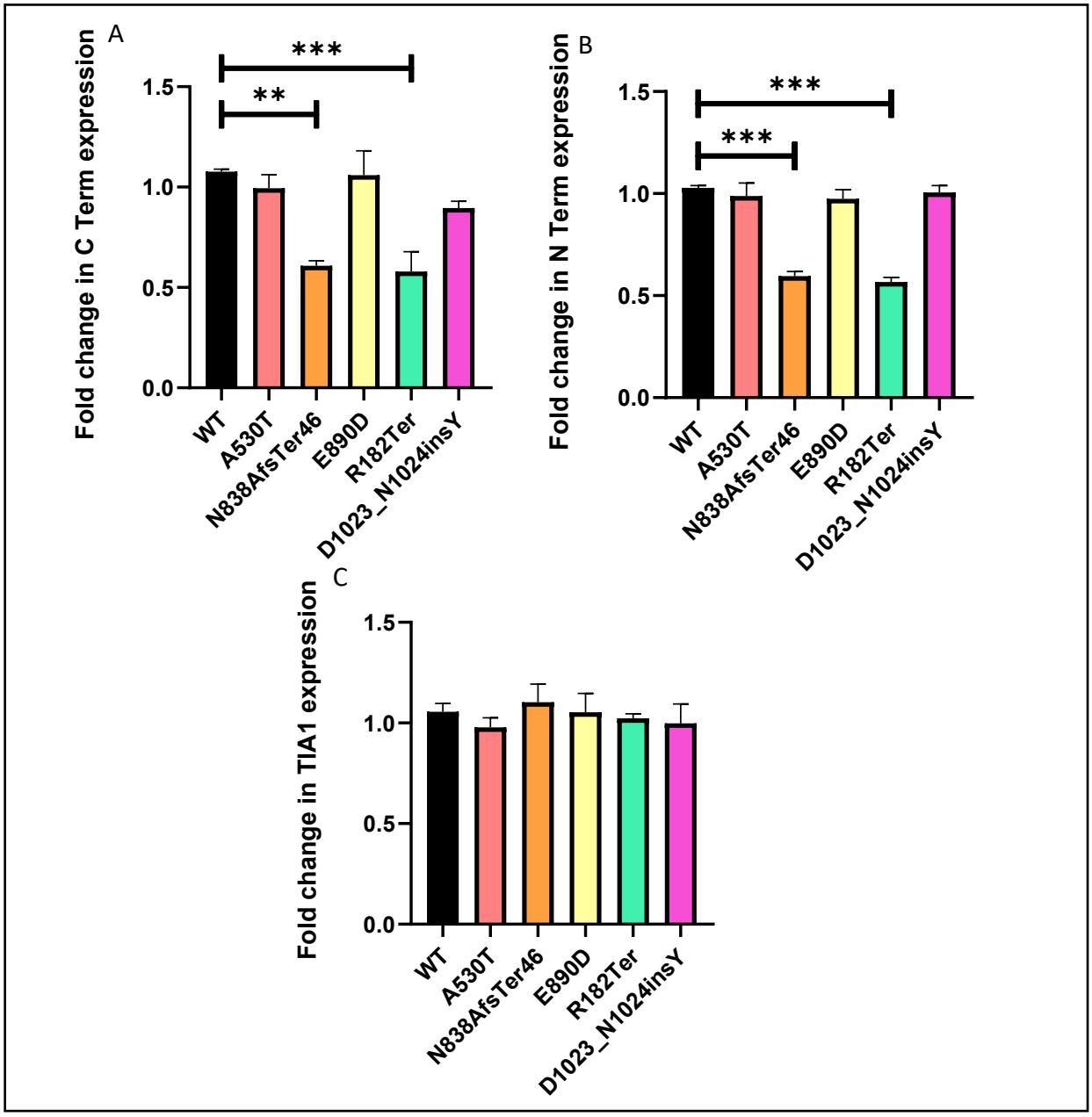

Figure 2. Mutants undetectable by immunoblotting exhibit reduced mRNA levels in HEK293 cells transfected with mutant constructs. (A) Fold change in the expression of the PDE10A C-terminus, data presented as mean ± SEM, statistical analysis was performed by one-way ANOVA followed by Dunnett's post hoc (**P < 0.001; n = 3). (B) Fold change in the expression of the PDE10A N-terminus in statistical analysis was performed by one-way ANOVA followed by Dunnett's post hoc (***P < 0.0001; n = 3). (C) Fold change in the expression of TIA-1 statistical analysis was performed by one-way ANOVA followed by Dunnett's post hoc, no significant differences were detected among the groups (P > 0.05; n = 3)

PDE10A Mutant Compartmentalisation and Localisation

The correct subcellular compartmentalization of PDE10A is crucial for its proper function and any disruption in its location and distribution within the cell is likely to decrease activity and result in a pathogenic phenotype. While the two key sites for the correct palmitoylation of PDE10A are present in most of the mutants, it is possible that some of the resulting amino acid sequence changes could sufficiently alter the protein's tertiary structure, impeding this post-translational modification. For instance, the Cys11 residue might not be accessible for palmitic acid attachment, or the site responsible for zDHHC recruitment might not be fully available.

To investigate these possibilities and assess the subcellular compartmentalization and morphology of the detectable mutants, confocal microscopy coupled with immunofluorescence staining was performed on HEK293 cells. This allowed to generate high-resolution images displaying the subcellular distribution of the FLAG-tagged mutants. R182Ter and Asn838AlafsTer46 were excluded from this analysis due to their undetectable expression levels. Upon visual inspection, cells transiently expressing A530T, E890D, and D1023_N1024insY PDE10A mutants exhibited no significant qualitative morphological differences compared to those expressing WT PDE10A (see figure 3A). Importantly, irrespective of their known pathogenicity, all cells transiently expressing these mutants presented similarly. There was no appreciable formation of aggregates such as P-bodies or SGs, which are often indicative of protein misfolding and cellular stress responses.

Consistent Membrane Distribution Across Mutants

Beyond qualitative visual assessment, the distribution of PDE10A across the membrane also fell within a consistent range for all the mutants and wild-type PDE10A. To quantitatively assess the presence of PDE10A at the membrane, the Total Corrected Cell Fluorescence (CTCF) of the imaged cells was determined, and the percentage localized to the membrane was calculated. The percentage of PDE10A localized to the membrane relative to the rest of the cell

was 50.25% for WT PDE10A. For the mutants, these values were 46.03% for A530T, 49.00% for E890D, and 45.80% for D1023_N1024insY. Crucially, no mutant displayed a significant difference in the concentration of PDE10A on the membrane. Both WT PDE10A and the non-pathogenic control mutant E890D showed very similar membrane localization to the pathogenic mutants A530T and D1023_N1024insY (see figure 3B).

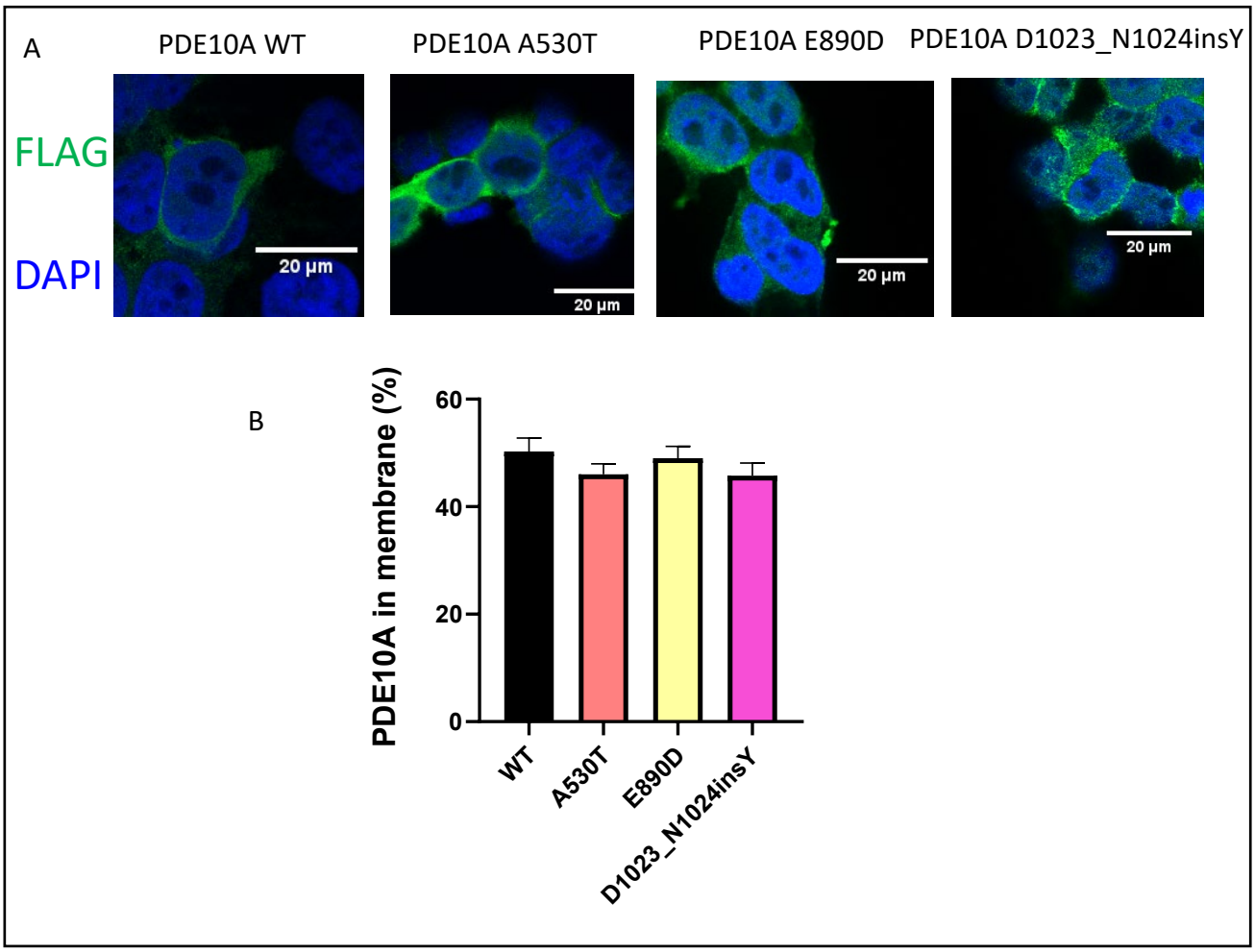

Figure 3. **Immunoblot-detectable mutants of PDE10A exhibit similar cellular localization to each other**. (A) Confocal microscopy images of HEK293 cells transfected with FLAG-tagged PDE10A constructs. FLAG-PDE10A is shown in green, and nuclei (DAPI) are in blue. (Scale bar 20 µm). (B) Corrected Total Cell Fluorescence (CTCF) analysis of PDE10A signal at the membranes of transfected HEK293 cells, comparing mutant forms relative to wild-type (WT) PDE10A. Data are presented as mean ± SEM. Statistical analysis was performed by one-way ANOVA, no significant differences were detected among the groups ($P > 0.05$; $n = 22$). Antibodies from Table 1 (1) and (9) were used.

In addition to quantification of fluorescence, subcellular fractionation of transiently transfected cells was performed in order to obtain a more direct and

accurate biochemical method of measuring the presence of PDE10A in the membrane and the cytosol. The transfected HEK293 cells were fractionated after harvesting using a commercial fractionation kit, allowing for the isolation of distinct cytosolic and membrane fractions. These fractions were then prepared for immunoblotting, similar to the previously analysed cell lysates. Each of these fractions was normalized to a loading control specific to that cellular compartment for accurate comparison. When examining the immunoblots, the previously established trend continued, with all detectable mutants displaying bands for PDE10A in both the membrane fraction and the cytosolic one. Densitometric analysis, used to quantify PDE10A presence in each fraction, showed that all groups maintained higher levels of PDE10A in the membrane fraction and lower levels in the cytosolic ones. Both pathogenic mutants (A530T and D1023_N1024insY) exhibited a ratio of PDE10A levels in their membrane relative to that in the cytosol very similar to that of WT PDE10A and the control non-pathogenic mutant E890D (see figure 4).

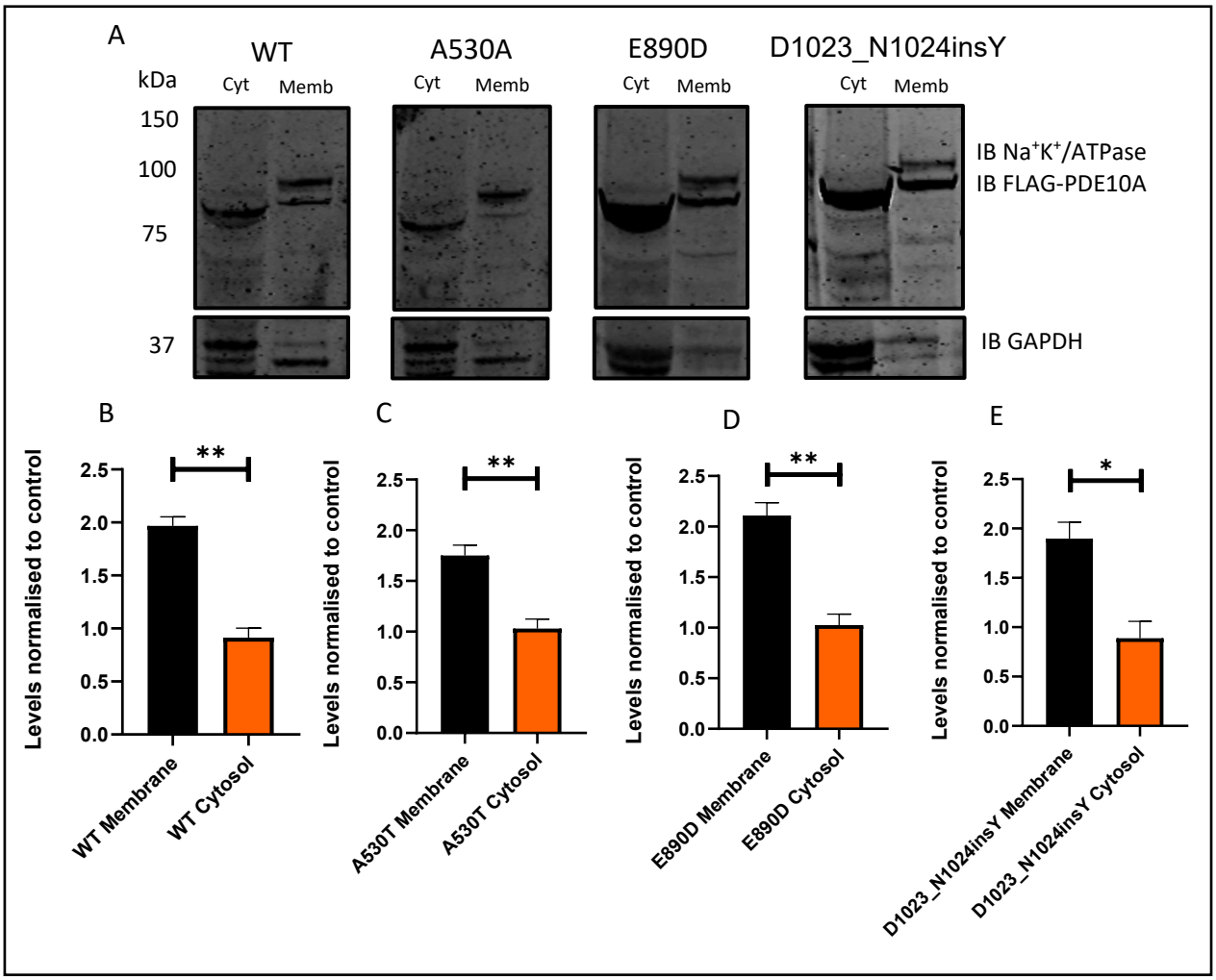

Figure 4. **Immunoblot-detectable PDE10A mutants show comparable cytosolic and membrane expression levels to wild-type.** (A) Immunoblot analysis of FLAG-tagged PDE10A protein constructs in fractionated HEK293 cells. GAPDH was used as a loading control for the cytosolic (Cyt) fraction, and Na$^+/K^+$ ATPase for the membrane (Memb) fraction. (B) Densitometric quantification of WT PDE10A levels in cytosolic and membrane fractions, normalized to respective loading controls (GAPDH for cytosol and Na^+/K^+ ATPase for membrane). (C) Densitometric quantification for the A530T mutant, normalized as in (B). (D) Densitometric quantification for the E890D mutant, normalized as in (B). (E) Densitometric quantification for the D1023_N1024insY mutant, normalized as in (B). For panels B-E, data are presented as mean ± SEM. A Welch's t-test was performed for each construct to assess the significance of the difference between cytosolic and membrane fractions. A significant difference was observed in the cytosolic and membrane distribution for WT and all indicated mutants, with consistent ratios across constructs (*P* **< 0.001, *P* *< 0.05; n = 3). Antibodies from table (1), (3), (4), (6) were used.

Absence of Gross Misfolding and Cellular Stress Responses

These findings provide evidence that, for the detectable PDE10A mutants (A530T, E890D, and D1023_N1024insY), neither aberrant protein aggregation nor mislocalisation appear to be primary mechanisms contributing to their pathogenicity or loss of function. Instead, the functional defects for these mutants likely stem from more subtle changes within the active site or regulatory domains that impact catalytic activity without compromising overall protein folding or trafficking.

The absence of characteristic aggregates such as SGs and P-bodies, and the lack of other stress-related morphological changes, strongly suggest that the transiently expressed PDE10A mutants do not induce a widespread or chronic ER stress response. This suggests that whatever effect these point mutations are having on PDE10A's structure, it is not severe enough to trigger a robust Unfolded Protein Response (UPR) critical for protein degradation via the proteasome or to induce the associated morphological changes. These results underscore that the cell's pathways responsible for protein synthesis, trafficking, and membrane anchoring largely remain functional for these variants, regarding of pathogenicity. The lack of differences in both morphology and compartmentalization makes them unreliable determinant factors for pathogenicity in the context of the mutants examined here, unlike in other investigations previous to this one.

Assessment of PDE10A Enzymatic Activity

Detection of the PDE10A mutants via immunoblotting, coupled with quantification of their cellular mRNA levels, offered no immediate insight into the specific mechanisms underpinning their pathogenicity. Furthermore, the mutants that could be successfully detected by these methods displayed no discernible morphological changes (at least at a visually identifiable scale through confocal microscopy images). Moreover, there appeared to be no significant deviation from WT PDE10A in the subcellular localization of any of the mutants (both pathogenic and non-pathogenic). To gain a more comprehensive understanding of how these mutations might affect PDE10A's function, a series of cAMP radioassays were performed. This approach was particularly relevant given that a majority of the studied mutants, especially those successfully detected via immunoblotting, are located within the active site of PDE10A. These assays quantitatively measured the phosphodiesterase activity of each mutant, which was compared to that of WT PDE10A,

Overall PDE Activity Profile of Mutants

When comparing the PDE activity of all observed mutants relative to that of WT PDE10A, all of the mutants exhibited lower levels. Interestingly, the non-pathogenic mutant E890D, which was used as a negative control, exhibited activity levels lower than those of WT PDE10A, despite not resulting in any of the observed hyperkinetic symptoms in individuals (see figure 5). This indicates that despite reduced activity when compared to the baseline established by the wild type, a complete loss of function is not a necessary outcome of every mutation. Therefore, E890D might be affecting the efficiency of PDE10A in hydrolyzing cAMP in a non-critical manner, reducing overall activity levels while allowing for overall function to remain physiologically sufficient.

Activity of Undetectable Mutants: R182Ter and Asn838AlafsTer46

In accordance with what would be expected for Asn838AlafsTer46 and R182Ter, their PDE activity compared to that of WT PDE10A is negligible (see figure 5). For R182Ter, even if it were not degraded via Nonsense-Mediated mRNA Decay (NMD), it would be structurally impossible for it to exhibit any hydrolysing

activity due to the complete absence of an active site capable of catalysing the reaction. Similarly, it would not be possible for Asn838AlafsTer46 to exhibit any PDE activity because approximately half of its catalytic domain is missing. There is a possibility that these lower activity levels are also due to an overall lower expression of the corresponding protein product. The minimal levels of PDE activity for both R182Ter and Asn838AlafsTer46 provide indirect evidence that these mutant proteins are not expressed at functionally relevant levels, but it would be necessary to confirm that NMD is occurring to be certain.

Activity of Pathogenic Mutants: A530T and D1023_N1024insY

In contrast to E890D, the pathogenic mutants A530T and D1023_N1024insY, which until now showed no variance from WT or E890D, now exhibit a much lower PDE activity than either of them, in the same negligible range as the early termination mutants (R182Ter and Asn838AlafsTer46) (see figure 5). It is reasonable to assume that both A530T and D1023_N1024insY result in a profound loss of function in PDE10A, effectively rendering it inactive.

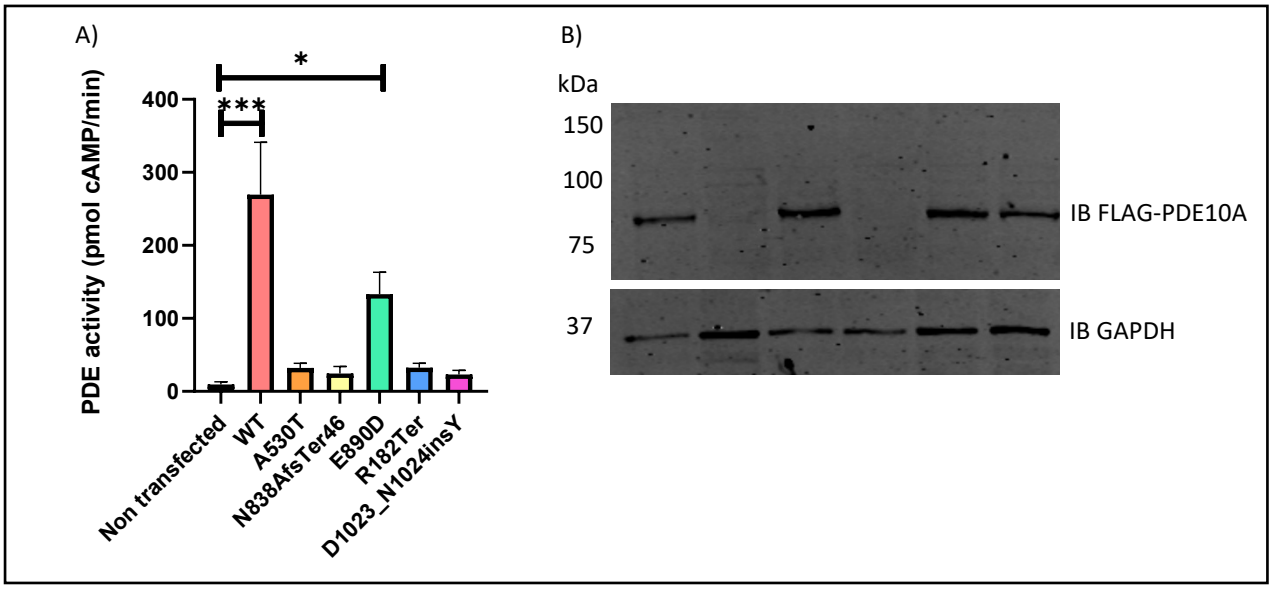

Figure 5. All pathogenic mutants exhibited significantly lower PDE activity compared to wild-type (WT) PDE10A while the non-pathogenic mutant showed a less extreme decrease in activity. A) Radioisotopic assay measuring PDE activity in HEK293 cells transfected with PDE10A constructs. Data are presented as mean ± SEM relative to values obtained for PDE10A WT. Statistical analysis was performed by **one-way ANOVA** followed by **Dunnett's post hoc test** (***P < 0.0001, *P < 0.05; n = 3) B) Immunoblot showing the protein levels of recombinant FLAG-tagged PDE10A constructs expressed in HEK293 cells. GAPDH was used as a loading control. Antibodies from Table 1 (2), (3), (6) and (8) were used

Discussion

The biochemical characterization of these newly identified PDE10A mutants has provided a series of key insights into the mechanisms contributing to the development of pathogenic phenotypes in affected individuals. For the early termination mutants, R182Ter and Asn838AlafsTer46, the consistent absence of detectable protein by immunoblotting, coupled with significantly reduced mRNA levels, presents possible explanation for their pathogenicity. A similar scenario can be observed in the case of PDE8B, where early termination mutants that produce a truncated protein (albeit detectable via immunoblotting), lead to lower levels of activity. This truncated PDE8B has been linked to the development of Autosomal-Dominant Striatal Degeneration, another CNS disorder (Appenzeller et al., 2010). PDE11A dysfunctional truncated mutants have been similarly linked with disease, as they have been found to be associated with adrenocortical hyperplasia and formation of adenomas (Horvath, Boikos, et al., 2006; Horvath, Giatzakis, et al., 2006).

In the case of R182Ter, termination occurs relatively early in the mRNA sequence, at the codon corresponding to amino acid 182. Conversely, Asn838AlafsTer46 is a frameshift mutation located near the end of the protein's coding sequence, causing termination at what would be residue 884. A well-established cellular mechanism where mRNA transcripts containing a premature stop codon (PTC), which are often a consequence of such early termination mutations, are recognized and subsequently degraded through a critical quality control pathway is known as Nonsense-Mediated mRNA Decay (NMD). In this process, a multi-protein complex known as the Exon Junction Complex (EJC) binds to mRNA upstream, typically 20-24 bases, of its exon-exon junctions. During a preliminary round of translation, often referred to as the "pioneer round," ribosomes traverse the mRNA sequence, displacing the EJCs as they proceed and translate the codons. However, if a PTC is encountered by the ribosome, usually located more than 50 amino acids upstream of an EJC, translation is halted. Crucially, the EJC remains bound to the mRNA at that

point. Upon this detection, the bound EJC initiates a precise recruitment process involving key NMD factors, primarily UPF proteins. These UPF proteins then trigger a cascade reaction that ultimately leads to the rapid decay of the mRNA transcript containing the PTC. It is possible that both R182Ter and Asn838AlafsTer46 are recognized as containing a PTC within their respective mRNA sequences due to being early termination mutants and subjected to NMD. This might explain why neither R182Ter nor Asn838AlafsTer46 were observed during immunoblotting, regardless of what antibody was used for probing, and why they exhibited significantly lower mRNA levels in the RT-qPCR analysis.

Findings in my investigation demonstrate that a possible mechanism underlying the non-functionality of early termination mutants, and subsequent contribution to hyperkinetic symptoms is severely low levels of protein product within the cell due to NMD. The presence of premature termination codons in the mRNA transcripts of both R182Ter and Asn838AlafsTer46 renders them vulnerable to NMD. Consequently, the reduced abundance of their respective mRNA transcripts, serves as quantitative evidence for the absence of these mutant proteins at biologically relevant levels. A different example is seen again in PDE8B where a mutant leading to the early termination of the enzyme, where NMD is suspected to occur, has been linked to adrenal tumours (Rothenbuhler et al., 2012). For these specific mutations, the onset of chorea-like symptoms, and the observed conditions in the other examples cited is not due to misfolding, altered localization, or aggregation of the protein. PDEs are either present but in a inactive way due to truncation, or directly eliminated via NMD, making early termination mutations in PDEs a probable marker for disease.

There remains a possibility that, in the case of the undetected mutants, even if at minimal levels, the protein is still expressed within the cell, and that even if truncated, the Ubiquitin-Proteasome System (UPS) might not efficiently tag them for efficient degradation. If this were to be the case, they would still be

present in cells, even if not be detected via immunoblotting, but still resulting in a pathogenic phenotype. In the case of R182Ter, the vast majority of the protein is not translated, with only a short segment of the GAF-A domain being the last section synthesized. Consequently, GAF-B, the other crucial regulatory region, is completely absent in the resulting product. More critically, the essential active site of the enzyme is also not translated. The resulting product for R182Ter is therefore a very short protein fragment, where its predicted complete lack of enzymatic activity is due to the absence of domains fundamental for proper protein function. Nonetheless, this is purely speculative, since during my investigation I did not have the means available to either generate a construct with the FLAG tag on the N-terminus or a working N-terminus antibody

In contrast, the truncated product of Asn838AlafsTer46 does retain both key regulatory domains (GAF-A and GAF-B) and a substantial segment of amino acids (over 200 residues long) belonging to the active site. This expressed segment of the active site in Asn838AlafsTer46 contains several amino acids that are absolutely vital for the catalytic activity of PDE10A. These include the majority of the residues responsible for coordinating with the essential divalent metal ions (specifically His795, His829, and Asp830) and the amino acids crucial for binding with cAMP, its natural substrate. Despite these preserved elements, the majority of the PDE10A's catalytic domain is indeed truncated. Furthermore, other key peptide segments are missing. These include the amino acid (Asp939) that binds with one of the two metal ions, and another amino acid (Gln726) that directly interacts with cAMP. Additionally, there are other amino acids which are not present in the truncated Asn838AlafsTer46 protein that, while not directly binding to cAMP, interact with it via van der Waals forces. Their absence might be a key factor contributing significantly to the observed loss of function in the Asn838AlafsTer46 mutant, although this remains speculation, and actual structural data would offer more definitive answers. Therefore, regardless of detection via immunoblotting, there is plenty of evidence to ascertain that R182Ter and Asn838AlafsTer46 would not be active due to critical changes in their structure.

In contrast to the early termination mutants, the remaining variants (A530T, the non-pathogenic E890D, and D1023_N1024insY) were consistently expressed at protein levels close to wild-type PDE10A, albeit slightly lower (including E890D), and their mRNA transcript levels also mirrored those of the wild-type. For these specific mutants, the overall protein expression level or mRNA abundance itself is not a decisive factor in determining their pathogenic or non-pathogenic nature. This is similar in a sense to the detectable truncated PDE8B mutants mentioned before, and also other mutant PDEs, such as PDE6A or PDE2A, where point mutations lead to a loss of function in the protein have been linked to the development of Retinitis pigmentosa (Appenzeller et al., 2010; Salpietro et al., 2018; Sothilingam et al., 2015).

This observed heterogeneity in the initial impact of these mutations on protein presence, ranging from a complete absence of protein due to mRNA degradation to normal protein expression levels, should inform the treatment of PDE10A related hyperkinetic disorders. With regards the treatment of other PDE-based pathologies, there are multiple directions in which therapies are being investigated. Modulation of Adenylyl Cyclases for example, seeks to regulate the levels of cyclic nucleotides by changing the activity of the proteins in charge of their synthesis. As such, the levels of cAMP and cGMP could be regulated depending on whether signalling is aberrant due to an increase or a decrease cyclic nucleotide levels (Tomczak et al., 2025). An example of an actual molecule used for these purposes is vericiguat, a chemical stimulator for a soluble guanylyl cyclase proven to improve primary outcomes in patients with Patients with Heart Failure and Reduced Ejection Fraction (Xia et al., 2022). On the other hand, inhibition of downstream of elements downstream of PDEs in the cAMP pathway is also a proposed form of therapy, where for example PKA inhibitors have been identified as a potential therapy in cancer and cardiovascular disease (Saad et al., 2018; Sapio et al., 2014). In addition, activation of PDE4 longforms has been achieved via a small allosteric molecule that phenocopies the PKA phosphorylation in its regulatory domain UCR1 (Omar et al., 2019). Although much of the research presented here is focused on the inhibition of PDEs in order to allow for an increase in cyclic nucleotide

levels, the same principles could be applied for a decrease, in order to make up for the lack of PDE10A activity. Specifically, the use of allosteric modulators to increase overall PDE activity might be a useful approach in the case of the investigated mutants. The allosteric activation of PDEs, specifically those that are membrane bound, found in the same MSNs which also contain PDE10A would increase PDE activity in the basal ganglia and, may rescue function. Since it is not necessary to increase activity to that of WT to see an improvement in symptoms, the upregulation of other PDEs could be done on a lower scale, which could prove beneficial in terms of side effects.

In the case of the detectable mutants (E890D, D1023_N1024insY, and A530T) no aberrant behaviour was observed in terms of compartmentalisation of the mutants. Cell morphology was also unaffected, with no visually identifiable changes that would indicate a significant cellular response. The lack of morphological and compartmentalisation changes is similar to that of other studies focusing other PDE10A mutants where despite severe changes. Nonetheless there is a notable number of cases where such aberrant behaviour occurs (Tejeda et al., 2020; Whiteley et al., 2019). The characterization of enzymatic activity has proven to be the more definitive criterion for elucidating pathogenicity among the expressed PDE10A mutants in this investigation. For the pathogenic mutants, A530T and D1023_N1024insY, the profound loss of PDE activity represents a determinant factor to the pathogenic phenotype. This severe functional impairment renders the enzyme inactive, incapable of efficiently hydrolysing cyclic AMP, disrupting the correct signalling of the second messenger. Such loss of function mutations where PDE10A levels remain stable, and localisation is normal are not uncommon both in PDE10A and other PDEs such as PDE4D. For example, mutations in the GAF-B domain lead to a loss in the cGMP stimulatory effect, resulting in lower activity, and leading to the childhood onset of chorea-like symptoms (Mencacci et al., 2016). When comparing to other proteins, such as PDE4D, a similar pattern can be observed, where are series of mutations in its UCR regulatory domain lead to decreased activity (H. Lee et al., 2012). These PDE4D mutants are then much more prone

to develop acrodysostosis, a condition characterised by skeletal malformations, resistance to hormones, and intellectual disability.

A similar situation can be seen when looking at the loss of activity mutants in this investigation. When looking at A530T, the mutated amino acid lies in very close proximity to the active site, which may explain the severe loss of function it incurs. In A530T, alanine, a short, non-polar, hydrophobic amino acid whose side chain is exclusively composed of a methyl group, is replaced by threonine, a slightly bulkier amino acid with a hydroxyl group in its side chain, making it hydrophilic (Worth & Blundell, 2010). Such an alteration is likely to affect both the local secondary structure and any surrounding catalytic activity.

A530T is located at the end of an alpha helix towards the interior of the protein. The change from a non-polar, smaller residue to a slightly bigger, hydrophilic one might induce structural stress in its immediate surroundings and contribute to partly destabilizing the helix. Such a conformational change, even if minor due to its close proximity to the active site, could impede the correct catalysis of the substrate by obstructing access to it or by forming unfavourable hydrogen bonds with nearby amino acids within the active site. Additionally, the newly introduced hydrophilic residue is capable of interacting with its surrounding amino acids, chemically disrupting PDE10A activity.

Due to the close proximity between the threonine at A530T and the active site, and the likely minor but critical disruption in structure, it is possible that this newly introduced hydrophilic residue interacts unfavourably with the proton-donating site, sequestering it and impeding the hydrolysis of cAMP by PDE10A. Although less likely, it is also conceivable that the change from a non-polar amino acid to a polar one containing a hydroxyl group significantly alters the local electrostatic environment, making the initiation of the catalytic reaction more difficult.

Furthermore, the threonine at A530T is also in very close proximity to the amino acids that coordinate with one of the two essential divalent metal ions of PDE10A, which it may also disrupt. Due to threonine being bulkier than alanine, it may cause steric interference, preventing proper interaction between the

coordinating amino acids and the metal cation. As the mutation might be causing slight conformational changes, as previously established, it could alter the geometry of the metal-binding pocket enough to make these coordinating amino acids unavailable to the cation. Additionally, the threonine itself might be disrupting the hydrogen bonding network necessary for the coordinating amino acids to properly bind with the cation, thereby reducing binding likelihood (Worth & Blundell, 2010).

Unlike A530T, D1023_N1024insY is located further away from the binding site of cAMP, much closer to the C-terminus of the protein. Unlike the previously discussed mutants, D1023_N1024insY should result in an insert mutation, where a tyrosine residue is added to the sequence, in between an aspartic acid and asparagine amino acids. The insert of tyrosine in between its surrounding amino acids, which themselves are located in an alpha helix, is very likely to cause extreme disruption to the secondary structure (Li et al., 2024). Since tyrosine is one of the bulkiest amino acids, and contains a large aromatic sidechain, with a polar hydroxyl group at the end, it is very likely to interfere with the hydrogen bonding backbone that stabilises the formation of the alpha helix. The major difference in size, relative to the surrounding amino acids, is also very like to cause massive steric hindrance to the secondary structure, which would be very unlikely to accommodate the newly inserted tyrosine and its bulky side chain. The inclusion of tyrosine would then be likely to cause major perturbation in the alpha helix structure, to the degree where local unwinding, a severe kink, or major disruption of the helical structure may occur. Whatever alterations in the structure of D1023_N1024insY are, they are not critical enough to alter its detection both via the FLAG and PDE10A antibodies when immunoblotting. Therefore, its stability in the context of it being tagged and degraded by the UPS is not greatly affected. It is most likely that the inserted tyrosine causes a structural distortion in PDE10A, stemming from the region where D1023_N1024insY is located. This disruption in the alpha helix where the insert is located is major enough to alter the conformation of either the active or binding sites in PDE10A. As a result, the enzyme is either unable to access its substrate, preventing hydrolysis, or even if it is able to access its substrate, the

reaction cannot be catalysed due to the active site becoming unavailable. Furthermore, such a substantial structural change could compromise the enzyme's conformational dynamics, hindering its ability to undergo the precise induced fit movements necessary for efficient substrate binding, catalysis, and product release during the catalytic cycle. Regardless of what is the specific structural explanation as to why D1023_N1024insY leads to a complete loss of PDE10A activity.

In the case of E890D, this mutant results in the replacement of glutamic acid (E) with aspartic acid (D) at position 890, within an alpha helix near the cAMP binding site. Specifically, glutamic acid has a longer side chain (by a single -CH2- residue) and a slightly higher pKa of 4.3, compared to aspartic acid, which is shorter and has a slightly lower pKa of 3.9 (Grimsley et al., 2008). While the region where E890D occurs is not in direct contact with cAMP, a portion of the helix immediately downstream is directly involved in substrate binding (Handa et al., 2008; Wang et al., 2007a). It is plausible that the subtle change from glutamic acid to aspartic acid affects the secondary structure of this alpha helix in a way that reduces the efficiency with which cAMP binds to PDE10A, while still allowing for a high enough level of activity. It is also possible that such a minor change in the length or flexibility of this specific alpha helix leads to reduced availability of the substrate to the active site, even if the binding affinity itself is not greatly affected. Determining such precise molecular occurrences would necessitate the application of structural biology methods, including the elucidation of the molecular structure of this specific mutant.

The investigation of the non-pathogenic mutant E890D helps achieve a better understanding of PDE10A and its functional landscape. Despite exhibiting lower phosphodiesterase activity compared to wild-type PDE10A (less than half on average), this variant does not result in the development of a pathogenic phenotype. E890D also shows overall decreased expression when compared to WT, at a p value very close to 0.05, even if non-statistically significant there is a trend that implies that lower activity might also be partly due to lower levels of

the enzyme. The non-pathogenic nature of E890D demonstrates that a specific threshold of residual enzymatic activity is physiologically sufficient to avert dysregulation of cyclic nucleotide signalling and onset of symptoms. Therefore, for the PDE10A mutants that are expressed within the cellular environment in this investigation, the level of enzymatic activity emerges as the principal determinant distinguishing pathogenicity from a non-pathogenic state. When looking at studies where heterozygous carriers still carry one WT allele for PDE10A, no aberrant phenotype is observed. These heterozygous carriers expressed a 70% reduction in striatal levels of PDE10A but did not show hyperkinetic symptoms. Rather than WT levels of activity being the necessary baseline for healthy individuals, there seems to a certain degree of tolerance for lower levels of hydrolysing activity, without that resulting in a pathogenic phenotype (Kalampokini et al., 2024). Additionally, mice Knock in (KI) studies have shown that generated heterozygous mutant mice with one WT and one mutant KI allele show very close levels of activity, CREB activation, and motor function, despite lower levels of protein expression (Diggle et al., 2016).

Nonetheless, there still have been cases in which heterozygous mutants having a clear pathogenic phenotype, indicating that depending on the mutation, it is possible to achieve a loss of function (Narayanan et al., 2018). In terms of understanding the treatment of hyperkinetic disorders where there is a lack of function for PDE10, the necessary levels for which activity has to be raised for function to be rescued may not need to be as high as WT PDE10A. While initial analysis did not offer immediate distinctions between pathogenic and non-pathogenic variants, the direct measurement of phosphodiesterase activity has proven to be a useful discriminator for those mutants successfully expressed and detected within the cell. The early termination mutants exhibited negligible PDE activity, which can mostly be attributed to their significantly reduced, if not absent, protein expression. In contrast, the non-pathogenic mutant E890D, despite being expressed at detectable levels, consistently showed lower PDE activity than WT PDE10A. However, this reduction in activity did not lead a pathogenic phenotype, indicating that a complete loss of activity may be necessary, and a certain residual activity level is physiologically sufficient.

Conversely, the pathogenic mutants A530T and D1023_N1024insY, which were expressed and localized in a virtually identical manner to WT PDE10A, displayed notably low PDE activity, reaching levels comparable to the early termination mutants and effectively rendering the enzyme inactive. This profound loss of function in A530T and D1023_N1024insY is attributed to specific structural alterations. These localized changes are proposed to induce structural stress, subtle conformational shifts, or disruption of key catalytic interactions without causing gross misfolding that would lead to protein degradation, which would have rendered them undetectable. Therefore, for those PDE10A mutants that are expressed and detected within the cell, a certain threshold of enzymatic activity seems to be the main factor determining their pathogenicity or non-pathogenicity. Such a threshold does not need to be too close to that of WT PDE10A, as the non-pathogenic mutant E890D, with PDE activity levels half of WT has not been reported to cause hyperkinetic symptoms. As such, the development of new therapies could be focused on reaching this threshold, without necessarily getting to the WT range.

This investigation's results collectively offer implications regarding the fundamental role of PDE10A in the onset and development of hyperkinetic disorders, adding further evidence to the hypothesis that PDE10A is critical for motor function. A prevailing notion that was mentioned in the introduction, states that changes in PDE10A levels, such as those observed in conditions like Huntington's Disease (HD), might represent a homeostatic, compensatory mechanism by the cell in response to neuronal stress or dysfunction. However, the characterization of these newly identified PDE10A mutants, in combination with previous genetic and biochemical studies indicate the contrary.

The consistent observation across all pathogenic PDE10A mutants in this study is that a severe impairment of functional PDE10A activity consistently correlates with the manifestation of hyperkinetic chorea-like symptoms. Whether this impairment stems from a profound quantitative deficiency in the enzyme's cellular presence, resulting from efficient mRNA degradation via NMD, or from a

severe qualitative reduction in its catalytic efficiency despite normal protein expression and subcellular localization, the outcome remains the same: the onset of hyperkinetic chorea-like symptoms similar to those of HD. The fact that the absence of functional PDE10A, irrespective of its specific molecular mechanism, consistently drives a pathogenic phenotype demonstrates that its proper function is not incidental or subject to compensatory downregulation. The evidence resulting of this investigation, however, indicate the precise opposite: the loss of functional PDE10A is likely to be the causative event. Such an event is observed not just with PDE10A, but multiple other PDEs, where both gain of function and loss of function mutations cause a pathogenic phenotype. This can be seen with PDE4D mutants, which as previously mentioned loss of function leads to acrosydostosis and has a negative impact on cardiovascular health (Lee et al., 2012; Lehnart et al., 2005). Mutants of other proteins in the family like PDE3A can lead to hypertension and brachydactyly, while PDE6 mutants as mentioned previously can cause retinitis pigmentosa (Bolger, 2021; Sothilingam et al., 2015). The fact that PDE10 is not the only protein in its superfamily to be responsible for a variety of disorders when mutated, shows that cyclic nucleotide signalling is a crucial element for a multitude of processes.

While the current investigation has provided specific insights into the pathogenic mechanisms of newly identified PDE10A mutants, the nature of PDE10A's physiological function and its role in hyperkinetic disorders necessitates further elaboration. A current gap in our understanding of these mutants concerns the atomic-level structural changes induced in some of these mutations. While the loss of activity in pathogenic mutants such as A530T and D1023_N1024insY have been proven, the exact structural changes that underpin these catalytic deficiencies, without leading to gross misfolding or mislocalisation, remain to be resolved. Elucidating the three-dimensional structures of these specific mutant proteins, and the non-pathogenic E890D, would provide insights into how these small conformational alterations within their active sites or regulatory domains impact substrate binding, catalysis, or protein kinetics. Such detailed structural information would allow for a more complete understanding of how these

mutations result in decreased PDE10A activity. For example, when studying mutants D674A and D564N for PDE10A, crystal structures of their active sites showed how a glutamine amino acid was locked in place, hindering substrate recognition (Wang et al., 2007). Additionally, more structural data, specific to each isoform of PDE10A, would be useful in understanding if mutations affect its ability to dimerise. It was mentioned previously that the different isoforms of PDE10A are able to both form homodimers, and in specific cases to for heterodimers with a different isoform, altering its subcellular localisation. Having a better understanding of how the ability of these mutants to dimerise is affected may be useful for explaining any changes in activity and phenotype.

For future RT-qPCR studies it would be helpful to include a mutant that does result in the formation of cellular aggregates in a morphologically distinct way. Such a mutant would be useful to make comparisons between it and all the other experimental groups, in order to have more certainty when looking at the mRNA levels for TIA1 between mutants. This would allow to first make sure that the formation of aggregates is correlated with an increase in TIA1 and then use that increase as indirect evidence of an increase in the formation of aggregates. Additionally, it would prove useful to directly assess if NMD is occurring, for example, by inhibiting NMD and measuring mRNA levels afterwards to check for rescue of mRNA levels of these mutants. On a similar note, generation of constructs with a FLAG tag on the N terminus, rather than the C terminus, would be an effective method to be able to better discern lack of expression of early termination mutants from lack of detection,

Finally, while the use of human embryonic kidney (HEK293T) cells provided an efficient system for initial biochemical characterization, the findings warrant validation and further exploration within more physiologically relevant contexts. HEK293T cells lack the same cell physiology and specific neuronal signalling pathways, characteristic of medium spiny neurons in the basal ganglia. Ideally future studies on these mutants, or similar ones, would make use of either primary neuronal cultures derived from relevant brain regions, or at least other established cell lines that resemble the basal ganglia more closely. Two possible cell lines to use in the future would be SH-SY5Y or N2a, as both are neuroblastoma cell lines that resemble MSNs better than HEK293, despite not

being as efficient regarding protein expression (Hergenhahn et al., 2024; Xicoy et al., 2017). Since SH-SY5Y is derived from human neuroblastoma, it endogenously expresses PDE10A, which might make it a more ideal cell line (Müller-Deubert et al., 2020). Such models would allow for the confirmation of these molecular findings within a more accurate environment more closely resembling the human brain. For the study of how PDE10A affects HD and its onset, it might be useful to use in vivo models such as zQ175 mice, which have already been used in HD studies where PDE10A was part of the focus (Häggkvist et al., 2017). This would allow to better understand if PDE10A disfunction directly contributes to the onset of HD, and if it has any effect on severity of symptoms.

Materials and Methods

Culture of HEK293 cells

HEK293 cells were cultured in Dulbecco's Modified Eagle's Medium (DMEM) supplemented with 10% foetal bovine serum (FBS), 100 U/ml penicillin and 100 µg/ml streptomycin (1% P/S) and incubated at 37 °C in a humidified atmosphere with 5% CO2. Cells were then transfected using Lipofectamine 3000 with the corresponding 3000 reagent according to the manufacturer's instructions. HEK293 cells had their media refreshed 24 hours after transfection with (DMEM) containing 10% FBS, 100 U/ml penicillin and 100 µg/ml streptomycin (1% P/S). HEK293 cells were harvested 48 hours post transfection for lysis.

Preparation and Imaging of Immunoblot Analysis

Lysis for HEK293 cells was done in 3T3 buffer (50 mM NaCl, 50 mM NaF, 25 mM HEPES, 5 mM EDTA, 30 mM sodium pyrophosphate, 10% glycerol, 1% Triton X-100; pH 7.5) supplemented with protease inhibitor tablets (Roche), then incubated for 30 min at 4 °C. After incubation lysates were centrifuged at 15,000 x g for 10 min at 4 °C, retaining the supernatants and discarding the resulting pellets. A Bradford assay was performed on the resulting supernatants and used to normalise for the lysates corresponding protein concentrations. Equal concentrations of protein samples were boiled in SDS loading buffer (10% SDS, 300mM Tris-HCl pH 7.2, 0.05% bromothymol blue, 10% β-mercaptoethanol) and 20–40 µg of each cell lysate were resolved on NuPAGE precast 4-12% gels (Invitrogen) followed by transfer to nitrocellulose membranes (Whatman). Nitrocellulose membranes were then blocked for 1 hour using LiCor Intercept blocking buffer for 1 hour at room temperature, membranes were then incubated with the relevant primary antibody overnight at 4 ºC. After primary antibody incubation membranes were then washed with TBST 3 times 10

minutes each and then incubated with the appropriate secondary antibody. After incubation with the secondary antibody the membranes were washed again with TBST 3 times 10 minutes each. For Immunoblot analysis nitrocellulose membranes were scanned on an LiCor Odyssey CLX-3000 imager, and then fluorescence levels of the relevant protein bands were quantified using Image Studio software v5.5.

Immunocytochemistry

HEK293 cells were fixed 24 h post-transfection with 4% paraformaldehyde for 10 minutes at room temperature. Coverslips were washed 3 times with PBS and incubated for 10 minutes with a permeabilising solution (0.2% Triton X-100). Cells were then incubated for an hour with a blocking solution (PBS supplemented with 1% BSA and 5% FBS). Afterwards, cells were incubated with the indicated primary antibodies diluted in blocking solution overnight at 4°C in a humidity chamber. Detection was performed using secondary antibodies conjugated to Alexa Fluor 488, and coverslips were mounted on glass slides with ProLong Gold with DAPI (ThermoFisher Scientific). All confocal images are single sections acquired using an inverted Zeiss Pascal LSM 510 confocal microscope.

Image analysis

Confocal images were analysed using ImageJ Fiji (NIH Image), Image intensity profiles were generated using the measure function available in ImageJ Fiji. For measurements of PDE10A enrichment at the plasma membrane in transfected HEK293 cells, both whole cells and their respective plasma membranes were measured individually. Intensity from whole membrane was calculated as the percentage relative to the signal obtained in the whole cell.

mRNA expression and quantification

RNA from transfected HEK293 cells was purified using the QIAGEN RNAeasy kit for RNA purification, with the included additional optional stage for DNA digestion. 2ug of total RNA were used as a template for cDNA synthesis with High-Capacity cDNA Reverse Transcriptase Kit (Applied Biosystems) according to the manufacturer's instructions. Real-time quantitative PCR was performed with SYBR green and the SYBR™ Green Universal Master Mix on the according to manufacturer's instructions when designing the heating curve, on a StepOne Plus Real-Time PCR System. Quantitative analysis was carried out using StepOne software Version 2.3 (Applied Biosystems), which calculated the threshold cycle (Ct) values. The relative gene expression of PDE10A was normalized by subtracting the Ct value of the endogenous control from the Ct value of the target assay for the average of each 2 well pair (for each respective condition) (ΔCt). The fold increase relative to a mock condition with no exogenous PDE10A expression was calculated using 2−ΔΔCT.

Subcellular fractionation

Harvested cells were fractionated using the Fraction-PREP Cell Fractionation Kit from abcam, according to manufacturer's instructions, with a series of adjustments. All indicated volumes of reagents were reduced by a magnitude of 0.25 to allow for a better protein concentration for easier detection in further analysis. At the end of the fractionation process three fractions were obtained in total, those being the membrane, cytosolic, and nuclear fractions. A Bradford assay was performed on the resulting fractions and used to normalise for the lysates corresponding protein concentrations. Equal concentrations of protein samples were boiled in SDS loading buffer (10% SDS, 300mM Tris-HCl pH 7.2, 0.05% bromothymol blue, 10% β-mercaptoethanol) and 20–40 µg of each cell lysate were resolved on NuPAGE precast 4-12% gels (Invitrogen) followed by transfer to nitrocellulose membranes (Whatman). Nitrocellulose membranes were then blocked for 1 hour using LiCor Intercept blocking buffer for 1 hour at room temperature, membranes were then incubated with the relevant primary antibody overnight at 4 ºC. A specific loading control was used in regard to each of the fractions to properly assess that fractionation was successful, choosing the housekeeping protein based on its presence in the relevant subcellular

location relative to the rest. After primary antibody incubation membranes were then washed with TBST 3 times 10 minutes each and then incubated with the appropriate secondary antibody. After incubation with the secondary antibody the membranes were washed again with TBST 3 times 10 minutes each. For Immunoblot analysis nitrocellulose membranes were scanned on an LiCor Odyssey CLX-3000 imager, and then fluorescence levels of the relevant protein bands were quantified using Image Studio software 5.5. When normalising protein fluorescence data of the band of interest, the specific loading control for the relevant fraction was used.

Phosphodiesterase activity assay

In order to determine Phosphodiesterase activity HEK293 cells were centrifuged at 500 x g for 10 minutes in 1.5 ml Eppendorf tubes, washed with PBS and centrifuged again. PBS was removed from the samples and KHEM buffer 50 mM KCl, 50 mM HEPES pH 7.2, 10 mM EGTA, 1.9 mM MgCl2) supplemented with protease and phosphatase inhibitor, at 4 ºC tablets was added to the resulting pellets, which were then lightly resuspended by pipetting up and down. The resulting samples were then positioned in a container with dry ice, and allowed to quickly freeze solid, once frozen the samples were thawed in a 37 ºC water bath until liquid. In between every freeze thaw cycle once lysate was thawed liquid, it was drawn and expelled repeatedly through a syringe with a 0.45 mm needle until fully resuspended again. The freeze-thaw cycle was repeated 5 times in total per sample, after which they were centrifuged at 13,000 x g 15 minutes at 4°C. The resulting supernatants were collected, and a Bradford assay was performed on them and used to normalise for the lysate's protein concentrations. The samples had [^{3}H] cAMP (Perkin Elmer) and standard cAMP added to them making up a 2 µM solution, then incubated at 30 ºC for 10 minutes, after which the reactions were terminated via incubation at 100 ºC and allowed to cool for a further 15 minutes. Once cooled the samples had snake (*Crotalus atrox*) venom added to them up to a concentration of 0.2 mg/ml and incubated at 30 ºC for an additional 10 minutes. Each sample then had 400 µl of activated resin (Dowex 1x8, pH 3, Sigma, 44340 as a 1:1:1 mixture of resin:water:ethanol) added to them. The samples with the resin were

vortexed periodically during 15 minutes and then centrifuged finally at 13,000 x g at 4 ºC for 5 minutes. After centrifugation 150 µL from the resulting supernatant of each sample was transferred to a scintillator vial, together with 1 ml of scintillant, mixed together, and then placed in a TRI-CARB 2900TR Liquid Scintillation Analyzer for measuring. The data obtained from the scintillator was then downloaded and analysed in order to obtain PDE activity from the measured CPMA counts. For this the following formula was used.

$$2.61 \times \frac{Average\ Value - Blank}{Average\ Total\ Count} \times 10 \times \frac{1000}{\mu g\ \text{Protein}}$$

Antibodies used in this investigation

Antibody	Supplier	Host	Dilution	Catalogue number	Application
(1) FLAG	Sigma	Mouse	1:2000 WB 1:500 IF	F3165	WB IF
(2) PDE10A	GeneTex	Rabbit	1:2000	GTX118886	WB
(3) GAPDH	Proteintech	Mouse	1:50000	60004-1-Ig	WB
(4) Na+Ka+ ATPase	DSHB	Mouse	1:3000	a6F	WB
(5) Lamin A/C	Proteintech	Rabbit	1:5000	10298-1-AP	WB
(6) IRDye 800CW Donkey anti-Mouse	LiCor	Donkey	1:20000	926-32212	WB
(7) IRDye 800CW Donkey anti-Rabbit	LiCor	Donkey	1:10000	926-32213	WB
(8) IRDye 680RD Goat anti-Rabbit	LiCor	Goat	1:10000	926-68071	WB
(9) Anti-mouse Alexa Fluor 488	Thermosfisher	Donkey	1:500	A32723	IF

Table 1

Plasmids for the constructs used in the investigation

Constructs were generated via site-directed mutagenesis of the base PDE10A with c-terminal FLAG tag construct from the 2020 Tejeda et. al paper previous to the start of the investigation by staff in the Baillie lab.

Construct	Source
pcDNA3.1 PDE10A1-WT-FLAG	Blue Sky BioServices
pcDNA3.1 PDE10A1-p.A530T-FLAG	Blue Sky BioServices
pcDNA3.1 PDE10A1-p.Asn838AlafsTer46-FLAG	Blue Sky BioServices
pcDNA3.1 PDE10A1-p.E890D-FLAG	Blue Sky BioServices
pcDNA3.1 PDE10A1-p.R182Ter-FLAG	Blue Sky BioServices
pcDNA3.1 PDE10A1-p. D1023_N1024insY -FLAG	Blue Sky BioServices

Table 2

List of primers used in this investigation

Primer name	Target	Primer sequence	Source
hPDE10A_qPCR_F1 (Forward)	N-terminal PDE10A	ATGGACCTTCTAATAATGCGAGC	Integrated DNA Technologies
hPDE10A_qPCR_R1 (Reverse)	N terminal PDE10A	TTCATCTGTCAAACTGGGGCT	Integrated DNA Technologies
hPDE10A_qPCR_F2 (Forward)	C terminal PDE10A	TGCCTGTGACCTTTGTTCTGT	Integrated DNA Technologies
hPDE10A_qPCR_R2 (Reverse)	N terminal PDE10A	TCATTTCATCACCCTCAGCCC	Integrated DNA Technologies

hTIA1_qPCR_F (Forward)	TIA1	GCCTAATGGTTGGCAAGTTCCTG	Integrated DNA Technologies
hTIA1_qPCR_R (Reverse)	TIA1	CCATTTTGCCCTTGAGGCGGTT	Integrated DNA Technologies
hGAPDH_qPCR_F (Forward)	GAPDH	GTCTCCTCTGACTTCAACAGCG	Integrated DNA Technologies
hGAPDH_qPCR_R (Reverse)	GAPDH	ACCACCCTGTTGCTGTAGCCAA	Integrated DNA Technologies

Table 3

Kits used in this investigation

Fraction-PREP Cell Fractionation Kit (Abcam, Catalogue number: ab288085), SYBR™ Green Universal Master Mix (Applied Biosystems, Catalogue number: 4309155), RNAeasy kit for RNA (Qiagen, Catalogue number: 74104), High-Capacity cDNA Reverse Transcription Kit Applied Biosystems, Catalogue number: 4368814)

Acknowledgement

This investigation would not have been possible without Professor George Baillie giving me the opportunity to develop my skills as a researcher in his lab, the wonderful supervision offered both by him and Dr. Angie Sin, and the support offered by all the members of the Baillie lab throughout my time there.

List of references

Ahmad, R., Bourgeois, S., Postnov, A., Schmidt, M. E., Bormans, G., Van Laere, K., & Vandenberghe, W. (2014). PET imaging shows loss of striatal PDE10A in patients with Huntington disease. *Neurology*, *82*(3), 279–281. https://doi.org/10.1212/WNL.0000000000000037,

Appenzeller, S., Schirmacher, A., Halfter, H., Bäumer, S., Pendziwiat, M., Timmerman, V., De Jonghe, P., Fekete, K., Stögbauer, F., Lüdemann, P., Hund, M., Quabius, E. S., Ringelstein, E.

B., & Kuhlenbäumer, G. (2010). Autosomal-Dominant Striatal Degeneration Is Caused by a Mutation in the Phosphodiesterase 8B Gene. *American Journal of Human Genetics*, *86*(1), 83–87. https://doi.org/10.1016/j.ajhg.2009.12.003

Baillie, G. S., Tejeda, G. S., & Kelly, M. P. (2019). Therapeutic targeting of 3',5'-cyclic nucleotide phosphodiesterases: inhibition and beyond. *Nature Reviews Drug Discovery 2019 18:10*, *18*(10), 770–796. https://doi.org/10.1038/s41573-019-0033-4

Beaumont, V., Zhong, S., Lin, H., Xu, W. J., Bradaia, A., Steidl, E., Gleyzes, M., Wadel, K., Buisson, B., Padovan-Neto, F. E., Chakroborty, S., Ward, K. M., Harms, J. F., Beltran, J., Kwan, M., Ghavami, A., Häggkvist, J., Tóth, M., Halldin, C., … Munoz-Sanjuan, I. (2016). Phosphodiesterase 10A Inhibition Improves Cortico-Basal Ganglia Function in Huntington's Disease Models. *Neuron*, *92*(6), 1220–1237. https://doi.org/10.1016/j.neuron.2016.10.064

Bolger, G. B. (2021). The PDE-Opathies: Diverse Phenotypes Produced by a Functionally Related Multigene Family. *Trends in Genetics*, *37*(7), 669–681. https://doi.org/10.1016/J.TIG.2021.03.002/ATTACHMENT/2C02068E-D5F2-4C56-B975-527804E4AC81/MMC1.DOCX

Cardinaux, J.-R., Notis, J. C., Zhang, Q., Vo, N., Craig, J. C., Fass, D. M., Brennan, R. G., & Goodman, R. H. (2000). Recruitment of CREB Binding Protein Is Sufficient for CREB-Mediated Gene Activation. *Molecular and Cellular Biology*, *20*(5), 1546. https://doi.org/10.1128/MCB.20.5.1546-1552.2000

Carecchio, M., & Mencacci, N. E. (2017). Emerging Monogenic Complex Hyperkinetic Disorders. *Current Neurology and Neuroscience Reports*, *17*(12), 97. https://doi.org/10.1007/S11910-017-0806-2

Chappie, T. A., Helal, C. J., & Hou, X. (2012). Current landscape of phosphodiesterase 10A (PDE10A) inhibition. *Journal of Medicinal Chemistry*, *55*(17), 7299–7331. https://doi.org/10.1021/JM3004976/ASSET/JM3004976.FP.PNG_V03

Charych, E. I., Jiang, L. X., Lo, F., Sullivan, K., & Brandon, N. J. (2010). Interplay of palmitoylation and phosphorylation in the trafficking and localization of phosphodiesterase 10A: Implications for the treatment of schizophrenia. *Journal of Neuroscience*, *30*(27), 9027–9037. https://doi.org/10.1523/JNEUROSCI.1635-10.2010,

Delnomdedieu, M., Tan, Y., Ogden, A., Berger, Z., & Reilmann, R. (2018). J06 A randomized, double-blind, placebo-controlled phase ii efficacy and safety study of the PDE10A inhibitor PF-02545920 in huntington disease (amaryllis). *Journal of Neurology, Neurosurgery & Psychiatry*, *89*(Suppl 1), A99–A100. https://doi.org/10.1136/JNNP-2018-EHDN.266

Demartinis, N., Lopez, R. N., Pickering, E. H., Schmidt, C. J., Gertsik, L., Walling, D. P., & Ogden, A. (2019). A proof-of-concept study evaluating the phosphodiesterase 10A Inhibitor PF-02545920 in the adjunctive treatment of suboptimally controlled symptoms of schizophrenia. *Journal of Clinical Psychopharmacology*, *39*(4), 318–328. https://doi.org/10.1097/JCP.0000000000001047,

Diggle, C. P., Sukoff Rizzo, S. J., Popiolek, M., Hinttala, R., Schülke, J. P., Kurian, M. A., Carr, I. M., Markham, A. F., Bonthron, D. T., Watson, C., Sharif, S. M., Reinhart, V., James, L. C.,

Vanase-Frawley, M. A., Charych, E., Allen, M., Harms, J., Schmidt, C. J., Ng, J., … Brandon, N. J. (2016). Biallelic Mutations in PDE10A Lead to Loss of Striatal PDE10A and a Hyperkinetic Movement Disorder with Onset in Infancy. *The American Journal of Human Genetics*, *98*(4), 735–743. https://doi.org/10.1016/J.AJHG.2016.03.015

Dong, J., Hawes, S., Wu, J., Le, W., & Cai, H. (2021). Connectivity and Functionality of the Globus Pallidus Externa Under Normal Conditions and Parkinson's Disease. *Frontiers in Neural Circuits*, *15*. https://doi.org/10.3389/FNCIR.2021.645287/PDF

Doyle, T. B., Hayes, M. P., Chen, D. H., Raskind, W. H., & Watts, V. J. (2019). Functional characterization of AC5 gain-of-function variants: Impact on the molecular basis of ADCY5-related dyskinesia. *Biochemical Pharmacology*, *163*, 169–177. https://doi.org/10.1016/J.BCP.2019.02.005

Ford, C. P. (2014). The Role of D2-Autoreceptors in Regulating Dopamine Neuron Activity and Transmission. *Neuroscience*, *282*, 13. https://doi.org/10.1016/J.NEUROSCIENCE.2014.01.025

Fujishige, K., Kotera, J., Michibata, H., Yuasa, K., Takebayashi, S. I., Okumura, K., & Omori, K. (1999). Cloning and characterization of a novel human phosphodiesterase that hydrolyzes both cAMP and cGMP (PDE10A). *Journal of Biological Chemistry*, *274*(26), 18438–18445. https://doi.org/10.1074/jbc.274.26.18438

Fujishige, K., Kotera, J., Yuasa, K., & Omori, K. (2000). The human phosphodiesterase PDE10A gene. *European Journal of Biochemistry*, *267*(19), 5943–5951. https://doi.org/10.1046/J.1432-1327.2000.01661.X

Furukawa, Y., Kaneko, K., Matsumoto, G., Kurosawa, M., & Nukina, N. (2009). Cross-seeding fibrillation of Q/N-rich proteins offers new pathomechanism of polyglutamine diseases. *Journal of Neuroscience*, *29*(16), 5153–5162. https://doi.org/10.1523/JNEUROSCI.0783-09.2009,

Galosi, S., Pollini, L., Novelli, M., Bernardi, K., Di Rocco, M., Martinelli, S., & Leuzzi, V. (2022). Motor, epileptic, and developmental phenotypes in genetic disorders affecting G protein coupled receptors-cAMP signaling. *Frontiers in Neurology*, *13*, 886751. https://doi.org/10.3389/FNEUR.2022.886751/BIBTEX

García, A. M., Brea, J., González-García, A., Pérez, C., Cadavid, M. I., Loza, M. I., Martinez, A., & Gil, C. (2017). Targeting PDE10A GAF Domain with Small Molecules: A Way for Allosteric Modulation with Anti-Inflammatory Effects. *Molecules : A Journal of Synthetic Chemistry and Natural Product Chemistry*, *22*(9), 1472. https://doi.org/10.3390/MOLECULES22091472

Gerfen, C. R. (2023). Segregation of D1 and D2 dopamine receptors in the striatal direct and indirect pathways: An historical perspective. *Frontiers in Synaptic Neuroscience*, *14*, 1002960. https://doi.org/10.3389/FNSYN.2022.1002960

Gines, S., Seong, I. S., Fossale, E., Ivanova, E., Trettel, F., Gusella, J. F., Wheeler, V. C., Persichetti, F., & MacDonald, M. E. (2003). Specific progressive cAMP reduction implicates energy deficit in presymptomatic Huntington's disease knock-in mice. *Human Molecular Genetics*, *12*(5), 497–508. https://doi.org/10.1093/HMG/DDG046,

Grimsley, G. R., Scholtz, J. M., & Pace, C. N. (2008). A summary of the measured pK values of the ionizable groups in folded proteins. *Protein Science : A Publication of the Protein Society*, *18*(1), 247. https://doi.org/10.1002/PRO.19

Häggkvist, J., Tóth, M., Tari, L., Varnäs, K., Svedberg, M., Forsberg, A., Nag, S., Dominguez, C., Munoz-Sanjuan, I., Bard, J., Wityak, J., Varrone, A., Halldin, C. and Mrzljak, L. (2017) 'Longitudinal Small-Animal PET Imaging of the zQ175 Mouse Model of Huntington Disease Shows In Vivo Changes of Molecular Targets in the Striatum and Cerebral Cortex', *Journal of Nuclear Medicine*, 58(4), pp. 617–622. doi: 10.2967/jnumed.116.180497.

Handa, N., Mizohata, E., Kishishita, S., Toyama, M., Morita, S., Uchikubo-Kamo, T., Akasaka, R., Omori, K., Kotera, J., Terada, T., Shirouzu, M., & Yokoyama, S. (2008). Crystal structure of the GAF-B domain from human phosphodiesterase 10A complexed with its ligand, cAMP. *Journal of Biological Chemistry*, *283*(28), 19657–19664. https://doi.org/10.1074/jbc.M800595200

Heckman, P. R. A., Van Duinen, M. A., Bollen, E. P. P., Nishi, A., Wennogle, L. P., Blokland, A., & Prickaerts, J. (2016). Phosphodiesterase Inhibition and Regulation of Dopaminergic Frontal and Striatal Functioning: Clinical Implications. *International Journal of Neuropsychopharmacology*, *19*(10), 1–16. https://doi.org/10.1093/IJNP/PYW030

Hergenhahn, L., Padutsch, N., Azawi, S., Weiskirchen, R., Liehr, T., & Rinčic, M. (2024). Cytogenomic Characterization of Murine Neuroblastoma Cell Line Neuro-2a and Its Two Derivatives Neuro-2a TR-Alpha and Neuro-2a TR-Beta. *Cells*, *13*(22), 1889. https://doi.org/10.3390/CELLS13221889/S1

Horvath, A., Boikos, S., Giatzakis, C., Robinson-White, A., Groussin, L., Griffin, K. J., Stein, E., Levine, E., Delimpasi, G., Hsiao, H. P., Keil, M., Heyerdahl, S., Matyakhina, L., Libè, R., Fratticci, A., Kirschner, L. S., Cramer, K., Gaillard, R. C., Bertagna, X., … Stratakis, C. A. (2006). A genome-wide scan identifies mutations in the gene encoding phosphodiesterase 11A4 (PDE11A) in individuals with adrenocortical hyperplasia. *Nature Genetics*, *38*(7), 794–800. https://doi.org/10.1038/NG1809,

Horvath, A., Giatzakis, C., Robinson-White, A., Boikos, S., Levine, E., Griffin, K., Stein, E., Kamvissi, V., Soni, P., Bossis, I., De Herder, W., Carney, J. A., Bertherat, J., Gregersen, P. K., Remmers, E. F., & Stratakis, C. A. (2006). Adrenal hyperplasia and adenomas are associated with inhibition of phosphodiesterase 11A in carriers of PDE11A sequence variants that are frequent in the population. *Cancer Research*, *66*(24), 11571–11575. https://doi.org/10.1158/0008-5472.CAN-06-2914,

Jäger, R., Russwurm, C., Schwede, F., Genieser, H. G., Koesling, D., & Russwurm, M. (2012). Activation of PDE10 and PDE11 phosphodiesterases. *Journal of Biological Chemistry*, *287*(2), 1210–1219. https://doi.org/10.1074/jbc.M111.263806

Jones-Tabah, J., Mohammad, H., Paulus, E. G., Clarke, P. B. S., & Hébert, T. E. (2022). The Signaling and Pharmacology of the Dopamine D1 Receptor. *Frontiers in Cellular Neuroscience*, *15*. https://doi.org/10.3389/FNCEL.2021.806618/PDF

Kalampokini, S., Xiromerisiou, G., Bargiotas, P., Anastasiadou, V. C., Costeas, P., & Hadjigeorgiou, G. M. (2023). PDE10A mutation as an emerging cause of childhood-onset hyperkinetic movement disorders: a review of all published cases. *Neuropediatrics*, *55*(4). https://doi.org/10.1055/A-2281-1822,

Kalampokini, S., Xiromerisiou, G., Bargiotas, P., Anastasiadou, V. C., Costeas, P., & Hadjigeorgiou, G. M. (2024). *PDE10A Mutation as an Emerging Cause of Childhood-Onset Hyperkinetic Movement Disorders: A Review of All Published Cases*. https://doi.org/10.1055/a-2281-1822

Knopp, C., Häusler, M., Müller, B., Damen, R., Stoppe, A., Mull, M., Elbracht, M., Kurth, I., & Begemann, M. (2019). PDE10A mutation in two sisters with a hyperkinetic movement disorder - Response to levodopa. *Parkinsonism and Related Disorders*, *63*, 240–242. https://doi.org/10.1016/j.parkreldis.2019.02.007

Knott, E. P., Assi, M., Rao, S. N. R., Ghosh, M., & Pearse, D. D. (2017). Phosphodiesterase Inhibitors as a Therapeutic Approach to Neuroprotection and Repair. *International Journal of Molecular Sciences*, *18*(4), 696. https://doi.org/10.3390/IJMS18040696

Kotera, J., Sasaki, T., Kobayashi, T., Fujishige, K., Yamashita, Y., & Omori, K. (2004). Subcellular Localization of Cyclic Nucleotide Phosphodiesterase Type 10A Variants, and Alteration of the Localization by cAMP-dependent Protein Kinase-dependent Phosphorylation. *Journal of Biological Chemistry*, *279*(6), 4366–4375. https://doi.org/10.1074/jbc.M308471200

Lanciego, J. L., Luquin, N., & Obeso, J. A. (2012). Functional Neuroanatomy of the Basal Ganglia. *Cold Spring Harbor Perspectives in Medicine*, *2*(12), a009621. https://doi.org/10.1101/CSHPERSPECT.A009621

Lau, J. K. C., Li, X. B., & Cheng, Y. K. (2010). A substrate selectivity and inhibitor design lesson from the PDE10-cAMP crystal structure: A computational study. *Journal of Physical Chemistry B*, *114*(15), 5154–5160. https://doi.org/10.1021/JP911156G/SUPPL_FILE/JP911156G_SI_001.PDF

Lee, D. (2015). Global and local missions of cAMP signaling in neural plasticity, learning, and memory. *Frontiers in Pharmacology*, *6*(Aug), 161. https://doi.org/10.3389/FPHAR.2015.00161/PDF

Lee, H., Graham, J. M., Rimoin, D. L., Lachman, R. S., Krejci, P., Tompson, S. W., Nelson, S. F., Krakow, D., & Cohn, D. H. (2012). Exome Sequencing Identifies PDE4D Mutations in Acrodysostosis. *American Journal of Human Genetics*, *90*(4), 746. https://doi.org/10.1016/J.AJHG.2012.03.004

Lehnart, S. E., Wehrens, X. H. T., Reiken, S., Warrier, S., Belevych, A. E., Harvey, R. D., Richter, W., Jin, S. L. C., Conti, M., & Marks, A. R. (2005). Phosphodiesterase 4D Deficiency in the Ryanodine-Receptor Complex Promotes Heart Failure and Arrhythmias. *Cell*, *123*(1), 25. https://doi.org/10.1016/J.CELL.2005.07.030

Li, C., Zheng, Y., & Jagodzinski, F. (2024). How pairs of insertion mutations impact protein structure: an exhaustive computational study. *Bioinformatics Advances*, *4*(1). https://doi.org/10.1093/BIOADV/VBAE138

Loughney, K., Snyder, P. B., Uher, L., Rosman, G. J., Ferguson, K., & Florio, V. A. (1999). Isolation and characterization of PDE10A, a novel human 3', 5'-cyclic nucleotide phosphodiesterase. *Gene*, *234*(1), 109–117. https://doi.org/10.1016/S0378-1119(99)00171-7

Macmullen, C. M., Vick, K., Pacifico, R., Fallahi-Sichani, M., & Davis, R. L. (2016). Novel, primate-specific PDE10A isoform highlights gene expression complexity in human striatum with

implications on the molecular pathology of bipolar disorder. *Translational Psychiatry 2016 6:2*, *6*(2), e742–e742. https://doi.org/10.1038/tp.2016.3

Marshall, R. D., Menniti, F. S., & Tepper, M. A. (2024). A Novel PDE10A Inhibitor for Tourette Syndrome and Other Movement Disorders. *Cells*, *13*(14), 1230. https://doi.org/10.3390/CELLS13141230

Mayr, B., & Montminy, M. (2001). Transcriptional regulation by the phosphorylation-dependent factor CREB. *Nature Reviews. Molecular Cell Biology*, *2*(8), 599–609. https://doi.org/10.1038/35085068

Mencacci, N. E., Kamsteeg, E. J., Nakashima, K., R'Bibo, L., Lynch, D. S., Balint, B., Willemsen, M. A. A. P., Adams, M. E., Wiethoff, S., Suzuki, K., Davies, C. H., Ng, J., Meyer, E., Veneziano, L., Giunti, P., Hughes, D., Raymond, F. L., Carecchio, M., Zorzi, G., … Bhatia, K. P. (2016). De Novo Mutations in PDE10A Cause Childhood-Onset Chorea with Bilateral Striatal Lesions. *American Journal of Human Genetics*, *98*(4), 763–771. https://doi.org/10.1016/j.ajhg.2016.02.015

Menniti, F. S., Chappie, T. A., & Schmidt, C. J. (2021). PDE10A Inhibitors—Clinical Failure or Window Into Antipsychotic Drug Action? *Frontiers in Neuroscience*, *14*, 600178. https://doi.org/10.3389/FNINS.2020.600178/XML/NLM

Miniaci, M. C., Speranza, L., Wolf, D., Ayon-Olivas, M., & Sendtner, M. (2024). BDNF-Regulated Modulation of Striatal Circuits and Implications for Parkinson's Disease and Dystonia. *Biomedicines 2024, Vol. 12, Page 1761*, *12*(8), 1761. https://doi.org/10.3390/BIOMEDICINES12081761

Mota, É., Bompierre, S., Betolngar, D., Castro, L. R. V., & Vincent, P. (2021). Pivotal role of phosphodiesterase 10A in the integration of dopamine signals in mice striatal D1 and D2 medium-sized spiny neurones. *British Journal of Pharmacology*, *178*(24), 4873–4890. https://doi.org/10.1111/BPH.15664

Müller-Deubert, S., Ege, C., Krug, M., Meißner-Weigl, J., Rudert, M., Bischof, O., Jakob, F., & Ebert, R. (2020). Phosphodiesterase 10A Is a Mediator of Osteogenic Differentiation and Mechanotransduction in Bone Marrow-Derived Mesenchymal Stromal Cells. *Stem Cells International*, *2020*, 7865484. https://doi.org/10.1155/2020/7865484

Narayanan, D. L., Deshpande, D., Das Bhowmik, A., Varma, D. R., & Dalal, A. (2018). Familial choreoathetosis due to novel heterozygous mutation in PDE10A. *American Journal of Medical Genetics, Part A*, *176*(1), 146–150. https://doi.org/10.1002/AJMG.A.38507,

Niccolini, F., Foltynie, T., Reis Marques, T., Muhlert, N., Tziortzi, A. C., Searle, G. E., Natesan, S., Kapur, S., Rabiner, E. A., Gunn, R. N., Piccini, P., & Politis, M. (2015). Loss of phosphodiesterase 10A expression is associated with progression and severity in Parkinson's disease. *Brain*, *138*(10), 3003–3015. https://doi.org/10.1093/BRAIN/AWV219,

Niccolini, F., Haider, S., Reis Marques, T., Muhlert, N., Tziortzi, A. C., Searle, G. E., Natesan, S., Piccini, P., Kapur, S., Rabiner, E. A., Gunn, R. N., Tabrizi, S. J., & Politis, M. (2015). Altered PDE10A expression detectable early before symptomatic onset in Huntington's disease. *Brain*, *138*(10), 3016–3029. https://doi.org/10.1093/BRAIN/AWV214

Omar, F., Findlay, J. E., Carfray, G., Allcock, R. W., Jiang, Z., Moore, C., Muir, A. L., Lannoy, M., Fertig, B. A., Mai, D., Day, J. P., Bolger, G., Baillie, G. S., Schwiebert, E., Klussmann, E., Pyne,

N. J., Ong, A. C. M., Bowers, K., Adam, J. M., … Henderson, D. J. P. (2019). Small-molecule allosteric activators of PDE4 long form cyclic AMP phosphodiesterases. *Proceedings of the National Academy of Sciences of the United States of America*, *116*(27), 13320–13329. https://doi.org/10.1073/PNAS.1822113116/-/DCSUPPLEMENTAL

Pérez-Dueñas, B., Gorman, K., Marcé-Grau, A., Ortigoza-Escobar, J. D., Macaya, A., Danti, F. R., Barwick, K., Papandreou, A., Ng, J., Meyer, E., Mohammad, S. S., Smith, M., Muntoni, F., Munot, P., Uusimaa, J., Vieira, P., Sheridan, E., Guerrini, R., Cobben, J., … Kurian, M. A. (2022). The Genetic Landscape of Complex Childhood-Onset Hyperkinetic Movement Disorders. *Movement Disorders*, *37*(11), 2197–2209. https://doi.org/10.1002/MDS.29182;PAGEGROUP:STRING:PUBLICATION

Rothenbuhler, A., Horvath, A., Libé, R., Faucz, F. R., Fratticci, A., Raffin Sanson, M. L., Vezzosi, D., Azevedo, M., Levy, I., Almeida, M. Q., Lodish, M., Nesterova, M., Bertherat, J., & Stratakis, C. A. (2012). Identification of novel genetic variants in phosphodiesterase 8B (PDE8B), a cAMP specific phosphodiesterase highly expressed in the adrenal cortex, in a cohort of patients with adrenal tumors. *Clinical Endocrinology*, *77*(2), 195. https://doi.org/10.1111/J.1365-2265.2012.04366.X

Russwurm, C., Jäger, R., Koesling, D., & Russwurm, M. (2011). Comparative analysis of PDE10A isoforms. *BMC Pharmacology*, *11*(Suppl 1), P56. https://doi.org/10.1186/1471-2210-11-S1-P56

Russwurm, C., Koesling, D., & Russwurm, M. (2015). Phosphodiesterase 10A is tethered to a synaptic signaling complex in striatum. *Journal of Biological Chemistry*, *290*(19), 11936–11947. https://doi.org/10.1074/JBC.M114.595769/ATTACHMENT/684A0230-2CF8-4090-AE2D-9E20BD2D4F74/MMC1.PDF

Saad, N. S., Elnakish, M. T., Ahmed, A. A. E., & Janssen, P. M. L. (2018). Protein Kinase A as a Promising Target for Heart Failure Drug Development. *Archives of Medical Research*, *49*(8), 530–537. https://doi.org/10.1016/J.ARCMED.2018.12.008

Salpietro, V., Perez-Dueñas, B., Nakashima, K., San Antonio-Arce, V., Manole, A., Efthymiou, S., Vandrovcova, J., Bettencourt, C., Mencacci, N. E., Klein, C., Kelly, M. P., Davies, C. H., Kimura, H., Macaya, A., & Houlden, H. (2018). A homozygous loss-of-function mutation in PDE2A associated to early-onset hereditary chorea. *Movement Disorders*, *33*(3), 482. https://doi.org/10.1002/MDS.27286

Sapio, L., Di Maiolo, F., Illiano, M., Esposito, A., Chiosi, E., Spina, A., & Naviglio, S. (2014). Targeting protein kinase A in cancer therapy: an update. *EXCLI Journal*, *13*, 843. https://pmc.ncbi.nlm.nih.gov/articles/PMC4464521/

Schmitt, J. M., & Stork, P. J. S. (2001). Cyclic AMP-Mediated Inhibition of Cell Growth Requires the Small G Protein Rap1. *Molecular and Cellular Biology*, *21*(11), 3671. https://doi.org/10.1128/MCB.21.11.3671-3683.2001

Sothilingam, V., Garrido, M. G., Jiao, K., Buena-Atienza, E., Sahaboglu, A., Trifunović, D., Balendran, S., Koepfli, T., Mühlfriedel, R., Schön, C., Biel, M., Heckmann, A., Beck, S. C., Michalakis, S., Wissinger, B., Seeliger, M. W., & Paquet-Durand, F. (2015). Retinitis pigmentosa: impact of different Pde6a point mutations on the disease phenotype. *Human Molecular Genetics*, *24*(19), 5486–5499. https://doi.org/10.1093/HMG/DDV275

Sotty, F., Montezinho, L. P., Steiniger-Brach, B., & Nielsen, J. (2009). Phosphodiesterase 10A inhibition modulates the sensitivity of the mesolimbic dopaminergic system to d-amphetamine: involvement of the D1-regulated feedback control of midbrain dopamine neurons. *Journal of Neurochemistry*, *109*(3), 766–775. https://doi.org/10.1111/J.1471-4159.2009.06004.X

Surmeier, D. J., Ding, J., Day, M., Wang, Z., & Shen, W. (2007). D1 and D2 dopamine-receptor modulation of striatal glutamatergic signaling in striatal medium spiny neurons. *Trends in Neurosciences*, *30*(5), 228–235. https://doi.org/10.1016/J.TINS.2007.03.008/ASSET/FB1ECE93-4F7A-4D51-B672-9FBECB1999EB/MAIN.ASSETS/GR1B3.JPG

Tejeda, G. S., Whiteley, E. L., Deeb, T. Z., Bürli, R. W., Moss, S. J., Sheridan, E., Brandon, N. J., & Baillie, G. S. (2020). Chorea-related mutations in PDE10A result in aberrant compartmentalization and functionality of the enzyme. *Proceedings of the National Academy of Sciences of the United States of America*, *117*(1), 677–688. https://doi.org/10.1073/PNAS.1916398117/SUPPL_FILE/PNAS.1916398117.SAPP.PDF

Threlfell, S., & West, A. R. (2013). Review: Modulation of striatal neuron activity by cyclic nucleotide signaling and phosphodiesterase inhibition. *Basal Ganglia*, *3*(3), 137. https://doi.org/10.1016/J.BAGA.2013.08.001

Tomczak, J., Kapsa, A., & Boczek, T. (2025). Adenylyl Cyclases as Therapeutic Targets in Neuroregeneration. *International Journal of Molecular Sciences 2025, Vol. 26, Page 6081*, *26*(13), 6081. https://doi.org/10.3390/IJMS26136081

Tong, H., & Gibb, A. J. (2008). Dopamine D1 receptor inhibition of NMDA receptor currents mediated by tyrosine kinase-dependent receptor trafficking in neonatal rat striatum. *The Journal of Physiology*, *586*(Pt 19), 4693. https://doi.org/10.1113/JPHYSIOL.2008.158931

Wang, H., Liu, Y., Hou, J., Zheng, M., Robinson, H., & Ke, H. (2007a). Structural insight into substrate specificity of phosphodiesterase 10. *Proceedings of the National Academy of Sciences of the United States of America*, *104*(14), 5782–5787. https://doi.org/10.1073/PNAS.0700279104/SUPPL_FILE/00279FIG5.JPG

Wang, H., Liu, Y., Hou, J., Zheng, M., Robinson, H., & Ke, H. (2007b). Structural insight into substrate specificity of phosphodiesterase 10. *Proceedings of the National Academy of Sciences of the United States of America*, *104*(14), 5782–5787. https://doi.org/10.1073/PNAS.0700279104/SUPPL_FILE/00279FIG5.JPG

Wang, H., Xu, J., Lazarovici, P., Quirion, R., & Zheng, W. (2018). cAMP Response Element-Binding Protein (CREB): A Possible Signaling Molecule Link in the Pathophysiology of Schizophrenia. *Frontiers in Molecular Neuroscience*, *11*, 382173. https://doi.org/10.3389/FNMOL.2018.00255/XML/NLM

Wanker, E. E., Ast, A., Schindler, F., Trepte, P., & Schnoegl, S. (2019). The pathobiology of perturbed mutant huntingtin protein–protein interactions in Huntington's disease. *Journal of Neurochemistry*, *151*(4), 507–519. https://doi.org/10.1111/JNC.14853;SUBPAGE:STRING:FULL

Wei, W., Ding, S., & Zhou, F. M. (2016). Dopaminergic treatment weakens medium spiny neuron collateral inhibition in the parkinsonian striatum. *Journal of Neurophysiology*, *117*(3), 987. https://doi.org/10.1152/JN.00683.2016

Whiteley, E. L., Tejeda, G. S., Baillie, G. S., & Brandon, N. J. (2019). PDE10A mutations help to unwrap the neurobiology of hyperkinetic disorders. *Cellular Signalling*, *60*, 31–38. https://doi.org/10.1016/J.CELLSIG.2019.04.001

Wilson, H., Niccolini, F., Haider, S., Marques, T. R., Pagano, G., Coello, C., Natesan, S., Kapur, S., Rabiner, E. A., Gunn, R. N., Tabrizi, S. J., & Politis, M. (2016). Loss of extra-striatal phosphodiesterase 10A expression in early premanifest Huntington's disease gene carriers. *Journal of the Neurological Sciences*, *368*, 243–248. https://doi.org/10.1016/J.JNS.2016.07.033

Worth, C. L., & Blundell, T. L. (2010). On the evolutionary conservation of hydrogen bonds made by buried polar amino acids: The hidden joists, braces and trusses of protein architecture. *BMC Evolutionary Biology*, *10*(1), 1–11. https://doi.org/10.1186/1471-2148-10-161/FIGURES/12

Xia, J., Hui, N., Tian, L., Liang, C., Zhang, J., Liu, J., Wang, J., Ren, X., Xie, X., & Wang, K. (2022). Development of vericiguat: The first soluble guanylate cyclase (sGC) stimulator launched for heart failure with reduced ejection fraction (HFrEF). *Biomedicine & Pharmacotherapy*, *149*, 112894. https://doi.org/10.1016/J.BIOPHA.2022.112894

Xicoy, H., Wieringa, B., & Martens, G. J. M. (2017). The SH-SY5Y cell line in Parkinson's disease research: a systematic review. *Molecular Neurodegeneration*, *12*(1), 1–11. https://doi.org/10.1186/S13024-017-0149-0/TABLES/3

Xie, Z., Adamowicz, W. O., Eldred, W. D., Jakowski, A. B., Kleiman, R. J., Morton, D. G., Stephenson, D. T., Strick, C. A., Williams, R. D., & Menniti, F. S. (2006). CELLULAR AND SUBCELLULAR LOCALIZATION OF PDE10A, A STRIATUM-ENRICHED PHOSPHODIESTERASE. *Neuroscience*, *139*(2), 597. https://doi.org/10.1016/J.NEUROSCIENCE.2005.12.042